# Aupouri Aquifer Groundwater Model

# Factual Technical Report - Modelling

WILLIAMSON WATER & LAND ADVISORY
WWA0091 | 2

21 March 2019

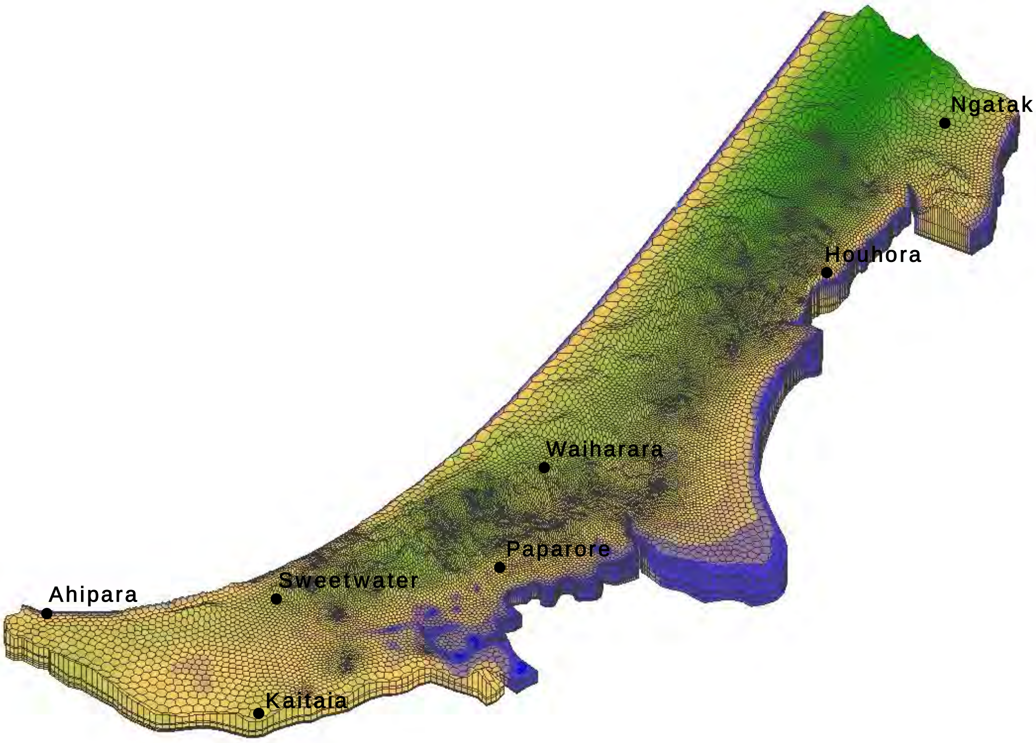

## Aupouri Aquifer Groundwater Model

| | |
|---|---|
| Project no: | WWA0091 |
| Document title: | Groundwater Modelling Analysis |
| Revision: | 2 |
| Date: | 21 March 2019 |
| Client name: | WWLA |
| Project manager: | Jon Williamson |
| Author(s): | Jacob Scherberg, Jon Williamson |
| File name: | G:\Team Drives\Projects\WSP-OPUS Consultants\WWA0091_Sweetwater Station Groundwater Take Consent Re-Configuration\Deliverables\DRAFT_Sweetwater_Groundwater_AEE_assessment.docx |

Williamson Water Advisory

PO Box 314,
Kumeu 0841,
Auckland
T +64 21 654422

### Document history and status

| Rev | Date | Description | By | Review | Approved |
|---|---|---|---|---|---|
| 1 | 5 March 2019 | Internal review | Jacob Scherberg | Louise Soltau | Jon Williamson |
| 2 | 21 March 2019 | Final Review | | | Jon Williamson |
| | | | | | |
| | | | | | |
| | | | | | |
| | | | | | |

### Distribution of copies

| Rev | Date issued | Issued to | Comments |
|---|---|---|---|
| 2 | 21 March 2019 | Public | |
| | | | |
| | | | |
| | | | |
| | | | |

## Contents

## Figures

# Executive Summary

Williamson Water & Land Advisory (WWLA) has undertaken the development of a numerical groundwater model for the Aupouri Aquifer, a shellbed aquifer located on the Aupouri Peninsula of Northland, New Zealand. The purpose of developing the Aupouri Aquifer Groundwater Model (AAGWM) was for evaluating the sustainability of proposed groundwater allocations. To facilitate this, the model compiles all existing information relating to hydrogeological conditions and water use on the Aupouri Peninsula.

The model was developed using the MODFLOW Unstructured Grid (MODFLOW-USG) developed by the United States Geological Survey (USGS) within the GMS10.2 modelling platform.

A conceptual model framework was developed based on a review of 198 bore logs within the model area. Bore logs were interpreted to characterise materials within a basic stratigraphic framework. Four primary layers were identified with their base elevations interpolated between the bore locations. The primary geologic layers used in the model are interbedded dune sand, weathered sand, peat and clay as an upper layer, followed by an upper shellbed, a layer of compact sand, and a lower shellbed. The shells beds comprise the primary aquifer in the model. The lower model boundary was determined by interpolating the elevation where basement rock was encountered as noted in bore logs.

The upper layer of the model was sub-divided into three layers to account for surface conditions and heterogeneity within the material. The upper model layers were classified into coastal sand, weathered sand, and clay/peat, based on soil types.

Climate data and water use data were evaluated to develop a time series data set for groundwater recharge and groundwater pumping.

Time series observations of groundwater levels were available from 56 bores. This data was the basis for model calibration. A steady state model was first calibrated to determine an initial estimate of parameter values and initial conditions for the transient model.

The model was calibrated in both steady state and transient modes, with the most weight given to transient calibration as this reflects long term temporal change. The mean of the RMSE for all gauges was 1.89 m, which is 7.1% of the observed range in groundwater head (26.5 m), while the RMSE for all groundwater level measurements used for model calibration was 2.10 m, or 7.9 % of the range of observations. A simulated RMSE of less than 10% of the measured range is considered a good calibration so both analysis criteria meet this standard. Temporal variability in groundwater levels was well simulated throughout the model while there was, in some cases, a discrepancy between simulated and observed groundwater elevation.

This report documents the methodology applied in the development of the AAGWM and presents the factual results of this modelling study.

# 1. Introduction

Williamson Water & Land Advisory (WWLA) has undertaken the development of a numerical groundwater model for the Aupouri Aquifer, a shellbed aquifer located on the Aupouri Peninsula of Northland, New Zealand. The purpose of developing the Aupouri Aquifer Groundwater Model (AAGWM) was for evaluating the sustainability of proposed groundwater allocations. To facilitate this, the model compiles all existing information relating to hydrogeological conditions and water use on the Aupouri Peninsula.

The Aupouri aquifer is managed by the Northland Regional Council and is divided into 10 allocation zones for management purposes, with the total amount of groundwater available for pumping within each management zone based on 15% of estimated total recharge for the given zone. The process of developing the AAGWM has entailed an assessment of both natural conditions and management practices related to the following aspects of the model area:

- Geologic and hydrogeologic conditions;
- Climate records over the past 60 years;
- Aquifer recharge based on rainfall and ground cover;
- Current and historic groundwater use;
- Surface water, including lakes, streams, and agricultural drains; and
- Coastal conditions with regard to ongoing or potential saline intrusion into the aquifer.

Consideration of these aspects of physical conditions within the Aupouri Peninsula were the basis for developing a conceptual framework that was used as the basis for the numerical model. A transient simulation of groundwater levels was calibrated to data from monitoring piezometers located within the model area. The resulting hydrological parameters were then considered in comparison to previous studies and known characteristics of the predominant materials that comprise the model domain. The calibrated model was then used to quantify the water balance for the entire Aupouri aquifer, making the model a tool that can be used to evaluate changes in the water balance that may result from management proposals or variability in climate.

This report is a comprehensive documentation of the methodology applied in the development of the AAGWM and presents the factual results of this modelling study. **Figure 1** presents the location of the model area and NRC groundwater management zones.

Figure 1. Project locality map. (See A3 attachment at rear).

## 1.1 Report Structure

The structure of this technical report is as follows:

- **Section 2** provides an overview of the conceptualisation of the groundwater flow model
- **Section 3** details the model construction and configuration.
- **Section 4** details the calibration of the steady-state and transient models**.**
- **Section 5** provides a summary of the key findings and conclusions of this project.

# 2. Model Conceptualisation

This section describes the conceptualisation of regional hydrogeological conditions and the methods applied in representing these conditions in the numerical groundwater flow model.

## 2.1 Soils

The western to central part of the project area is predominately comprised of sandy brown soils. Along both coastal strips there are coastal dunes, which are unconsolidated and windblown with little to no soil development and are excessively drained.

The eastern area is mixed with a variety of peat, sand and pockets of clay soils. The prevalent soils in the eastern areas are loamy peat and peaty sand. The loamy peat soils are organic, characterised by high water available capacity and low bulk density. The peat in these soils is moderately decomposed.

The peaty sand soils are pan podzols, which have cemented pans within the B horizon and have naturally low fertility and low permeability, limiting root depth.

It is interesting to note that most boreholes display units of peat and iron pan at multiple depths, suggesting the sand dune sequences have shifted in location and hence are highly dynamic through geological time.

Long-time local farmers and orchard developers provided the following anecdotal information on iron pans:

- "The iron pans vary in both thickness and number of layers" (pers. com. Stanisich, Broadhurst, Hayward).
- "There are multiple layers of pan at varying depths and our pan breaking for planting rows only seems to create vertical drainage at the top" (pers com. McClarnon).
- "Monitoring of bores screened in different zones during test pumping often show no effect at shallower levels to the pumping bore, indicating some separation of zones" (pers. com. Stanisich, Hayward).
- "From bore logs, iron pans are often recorded as consolidated brown sands. However, these may not be the only confining layers. Consolidated mica sands and silts are also good barriers" (pers. com. Stanisich).

## 2.2 Geology

The geology of the Aupouri Peninsula consists of Pleistocene and Holocene unconsolidated sedimentary materials deposited in beach and dune (abandoned shorelines and marine terraces) and associated alluvial, intertidal estuarine, shallow marine, lakebed and wetland environments.

The geologic units in the model domain were identified through the available bore logs sourced from NRC. The sediments near the surface typically comprise fine-grained sands, interspersed with sporadic iron pan, peat, lignite, silt, gravel and shellbeds.

With distance inland from the coast, the sand deposits become progressively older and have a higher degree of compaction and weathering compared to the younger foredune sands located at the coast.

With increasing depth, the occurrence of shellbed layers increases. The shellbeds comprise layers that typically range in composition from 30-90% medium to coarse shell and 10-70% fine sand. The shellbed aquifer typically resides from approximately 70 to 120 mBGL and is the most prolific water yielding aquifer in the region and hence the target for irrigation bores.

Underlying the shellbed aquifer are basement rocks of the Mount Camel Terrain, which typically comprise hard grey to dark green / black igneous rocks described in Isaac (1996) as intercalated basalt and basaltic andesite lava, pillow lava, rhyolitic tuff, tuff-breccia, with sedimentary deposits of conglomerate, sandstone and mudstone also present.

Drilling data from bores in the Aupouri aquifer indicates that the sedimentary sequence can be broadly classified into two lithological units. The upper bulk layer comprises the fine-grained sands, interspersed with iron pan, peat, lignite, and silt. The lower layer comprises mostly shellbeds, although recent drilling has identified the existence of two discrete shell units separated by a thin fine sand or silt layer, hence the lower layer is sub-divided into three distinct layers. The lithological unit classification developed for this study is exemplified in **Figure 2A** and **Figure 2B** using three reliable bore logs, and is described as follows:

- ***Layer 1 – Sand / Silt.*** A sequence of predominately unconsolidated fine sand intersperses with discontinuous layers of alternating iron pan, silt and peat. The layer varies in thickness from approximately 45 m to 110 m with the thickest regions located around the model area peak elevations.
- ***Layer 2 – Upper Shellbed.*** A sequence of shellbeds comprising medium to coarse shell with some fine sand in the matrix. The proportion of shell typically varies from 30% to 90%. The layer is typically encountered at a depth of 60 - 110 mBGL and varies in thickness from typically 5 m - 15 m.
- ***Layer 3 – Sand.*** A thin layer of finer sediment separating the upper and lower shellbed.
- ***Layer 4 – Lower Shellbed.*** A sequence of shellbeds typically comprising a higher proportion of shell with coarser grain size than the upper shellbed. In some locales, the shell is more consolidated and described by drillers as shell rock. Drillers also report circulation losses when drilling this formation. The layer is typically encountered at depths of 80 - 145 mBGL and varies in thickness from typically 5 m - 30 m.

**Honey Tree Farm Bore**
(Drilled on 20 June 2016)

| From (mBGL) | To (mBGL) | Lithology |
|---|---|---|
| 0 | 1 | Brown pan |
| 1 | 4 | Brown sands |
| 4 | 5 | White/green sands |
| 5 | 8 | Brown sands |
| 8 | 22 | Grey/brown Sands |
| 22 | 37.6 | Very fine green/grey sands |
| 37.6 | 38.4 | Brown silt |
| 38.4 | 40.1 | Grey silt |
| 40.1 | 42.2 | Fine brown/grey sands |
| 42.2 | 47 | Green/grey sandy silts |
| 47 | 58 | Green sandy silt- some shell |
| 58 | 58.9 | Cemented black sand |
| 58.9 | 60 | Shellbed 40% shell |
| 60 | 65 | Shellbed 70% shell |
| 65 | 68 | Coarse shells, gravels |
| 68 | 72.6 | 80% shell/coarse gravel 30mm |
| 72.6 | 72.8 | Silty sand |
| 72.8 | 82 | Fine sands, some shell |
| 82 | 83 | 10% shell/ sand |
| 83 | 110 | Consolidated shell - soft shell - rock |
| 110.3 | 110.7 | Grey soft rock |
| 110.7 | 111.6 | Harder black rock |

Model layers: Layer 1 - Sand/Silt; Layer 2 - Upper Shellbed; Layer 3 - Sand; Layer 4 - Lower Shellbed

**Mapua Orchard Bore**
(Drilled on 19 April 2017)

| From (mBGL) | To (mBGL) | Lithology |
|---|---|---|
| 0 | 6 | Brown dune sands |
| 6 | 12 | Green/grey sands |
| 12 | 15 | Black sandy peat/silts |
| 15 | 24 | Fine grey sands |
| 24 | 25 | Brown organic silts |
| 25 | 28 | Brown fine sand, silica |
| 28 | 29 | Peat/timber |
| 29 | 40 | Silica sands/brown sands |
| 40 | 44 | Fine grey sands/silica |
| 44 | 47 | Brown sands/organic silts |
| 47 | 48.5 | Grey sandy silt |
| 48.5 | 60 | Clean fine grey sands, Mica |
| 60 | 62 | Grey sands, flecks of organics |
| 62 | 82 | Dark grey sands, some black sand |
| 82 | 83.2 | Fine black/grey sand |
| 83.2 | 86 | 30% Medium shell |
| 86 | 87 | 50% Medium shell |
| 87 | 91 | 60% Medium shell |
| 91 | 94 | Fine sand, traces of shell |
| 94 | 97 | 60% Medium/ coarse shell, a few lenses of silt. Balance sand |
| 97 | 98 | 50% M/c blk shell |
| 88 | 99 | 60% M/c blk shell |
| 99 | 101 | 90% Medium/coarse black shell |
| 101 | 102 | Fine grey sand |
| 102 | 103 | 90% Coarse blk shell |
| 103 | 104 | 70% Coarse blk shell |
| 104 | 105 | 50% Coarse blk shell |
| 105 | 106 | 25% Coarse blk shell |
| 106 | 107 | 40% Coarse blk shell |
| 107 | 108 | 30% Coarse blk shell |
| 108 | 110 | Fine grey sand, shell fragments |
| 110 | 111.4 | 30% Coarse shell |
| 111.4 | 112 | Dark grey rock |

Model layers: Layer 1 - Sand/Silt; Layer 2 - Upper Shellbed; Layer 3 - Sand; Layer 4 - Lower Shellbed

**Largus Orchard Bore**
(Drilled on 12 April 2017)

| From (mBGL) | To (mBGL) | Lithology |
|---|---|---|
| 0 | 1 | Golden dune sand |
| 1 | 4.5 | Peat and timber |
| 4.5 | 18 | Brown/green fine sands |
| 18 | 42.7 | Grey/white sands |
| 42.87 | 45.5 | Firm grey sandy silts |
| 45.5 | 47 | Brown peaty silts |
| 47 | 53 | Brown/grey fine sands |
| 53 | 63 | Green/grey fine sands, some thin bands fine gravel |
| 63 | 67.5 | Sandy silt, flecks of shell |
| 67.5 | 68.5 | Cleaner silt, shell |
| 68.5 | 73 | Grey silt |
| 73 | 74.1 | Cleaner sand, shell |
| 74.1 | 76 | 60% Coarse shell |
| 76 | 77 | 20% Coarse shell |
| 77 | 78 | 50% Coarse shell |
| 78 | 80 | 20% Coarse shell |
| 80 | 83 | 70% Coarse shell |
| 83 | 84 | 50% Coarse/med shell |
| 84 | 86 | 50% Medium shell |
| 86 | 88 | 30% Medium shell |
| 88 | 89 | 50% Medium shell |
| 89 | 91 | 30% Medium shell |
| 91 | 93.6 | 50% Coarse/med shell |
| 93.6 | 93.8 | Light green silt |
| 93.8 | 105 | Firm, clean, grey/white shell rock |
| 105 | 106 | Softer mushy shell rock |
| 106 | 107 | Clean firm shell rock |
| 107 | 110.9 | Softer mushy shell rock |

Model layers: Layer 1 - Sand/Silt; Layer 2 - Upper Shellbed; Layer 3 - Sand; Layer 4 - Lower Shellbed

Figure 2A. Lithological unit classification from example borelogs.

**Valic-1**
(Drilled on 16 August 2006)

| From (mBGL) | To (mBGL) | Lithology | Model layers |
|---|---|---|---|
| 0 | 1 | Fine sand-brown | Layer 1 - Sand/Silt |
| 1 | 2 | Fine sand-dark brown | |
| 2 | 4 | Fine sand-light brown/grey | |
| 4 | 6 | Fine sand-light orange/brown | |
| 6 | 13 | Fine sand-light orange/brown. Trace organics | |
| 13 | 15.5 | Fibrous peat with wood/roots. Black | |
| 15.5 | 18 | Fine sand-dark brown/grey. Siliceous. Trace mica | |
| 18 | 20 | As above-becoming greyish brown | |
| 20 | 26 | Fine sand-dark brown/grey. Siliceous. Trace mica | |
| 26 | 29 | Amorphous peat, dark brown/black | |
| 29 | 33 | Fine sand, dark brown/brownish grey | |
| 33 | 45 | Fine sand, dark brown/brownish grey. Minor medium to coarse sand (quartz/silica). Trace mica | |
| 45 | 52 | Fine to medium sand-grey | |
| 52 | 56 | Medium sand, greyish brown. Minor coarse sand quartz/silica and mica | |
| 56 | 62 | Fine sand-orange brown | |
| 62 | 67 | Fine sand as above becoming grey | |
| 67 | 68 | Fine-med brown | |
| 68 | 75 | Fine sand , greenish grey, glauconitic, siliceous, minor mica | |
| 75 | 83 | Fine sand-greenish grey with minor mica; glauconitic, siliceous | |
| 83 | 85 | Fine sand as above. Trace fine shell | |
| 85 | 86 | As above, coarser shell | Layer 2 - Upper Shellbed |
| 86 | 88 | Fine grey sand. Coarse shell up to 40% | |
| 86 | 90 | Fine sand. 10% Coarse shell | |
| 90 | 93 | Silty fine sand with marine mud. Trace fine to coarse shell | Layer 3 - Sand |
| 93 | 98 | Silty fine sand with marine mud. Coarse shell 10-40% increasing with depth | Layer 4 - Lower Shellbed |
| 98 | 100 | Coarse granular shell (65%) with fine grey | |
| 100 | 108 | Fine sand, grey. 10% shell | |
| 108 | 117 | Fine sand, grey, trace shell | |

**George Ujdar Bore**
(Drilled on 06 April 2006)

| From (mBGL) | To (mBGL) | Lithology | Model layers |
|---|---|---|---|
| 0 | 5 | Topsoil/brown-grey sand | Layer 1 - Sand/Silt |
| 5 | 48 | Brown/grey sands | |
| 48 | 55 | Grey sand | |
| 55 | 74 | Brown Sand | |
| 74 | 87 | Compacted grey sand | |
| 87 | 92 | Brown sand with peate and shell | |
| 92 | 97 | Coarse shell | Layer 2 - Upper Shellbed |
| 97 | 101 | Fine shell with fine sand | Layer 3-Sand |
| 101 | 104 | Coarse shell | Layer 4-Lower Shellbed |
| 104 | 105 | Basement rock | |

**Sweetwater Monitoring Well 1**
(Drilled on 10 October 2007)

| From (mBGL) | To (mBGL) | Lithology | Model layers |
|---|---|---|---|
| 0 | 1 | Golden dune sand | Layer 1 - Sand/Silt |
| 1 | 6 | Peat and timber | |
| 6 | 25 | Fine brown sand/silt, well sorted | |
| 25 | 27 | Peat | |
| 27 | 30 | Sandy grey silt, trace shell (fine) | |
| 30 | 36 | Peat, black and fibous. Sand content increasing with depth | |
| 36 | 40 | Well sorted fine sand, increasingly silty with depth | |
| 40 | 46 | Clayey sand, fine, well sorted | |
| 46 | 48 | Fine shell | |
| 48 | 51 | Peat | |
| 51 | 74 | Grey sand, minor silt, clay and fine to medium shell | |
| 74 | 86 | Shell bed with minor sand, silt, and fine to medium gravels. Shell fraction 70-90% | Layer 2 - Upper Shellbed |
| 86 | 89 | Sandy shell with fine medium grey sand | Layer 3-Sand |
| 89 | 96 | Shell bed with fine grey sand, silt. Shell fraction 30-60% | Layer 4 - Lower Shellbed |
| 96 | 98 | Sandstone (hard, grey-basement rock) | |

Figure 2B. Lithological unit classification from example borelogs.

## 2.3 Aquifer Hydraulic Parameters

Groundwater is found throughout the unconsolidated sedimentary materials that occur within the model area, although these materials vary in their ability to store and transmit water, primarily due to grain size, cementation, weathering and compaction.

Test pumping and numerical modelling exercises for irrigation take resource consent applications have been undertaken over the years and summarised in the reports of HydroGeo Solutions (2000), SKM (2007a), SKM (2010), Lincoln Agritech (2015) and most recently by Williamson Water Advisory in 2017 (WWA, 2017). Data from these reports has been reproduced in tables provided **Appendix A**, and is summarised below in **Table 1** where it is presented in the context of our conceptual model as described in the previous section of this report.

Table 1. Summary of previously measured and modelled hydraulic properties for WWLA layer conceptualisation.

| Unit | $K_x$ (m/s) | | | S (-) | | |
|---|---|---|---|---|---|---|
| | Min | Max | Arithmetic Mean | Min | Max | Arithmetic Mean |
| Layer 1 - Sand / silt | $1.0x10^{-5}$ | $1.1x10^{-4}$ | $8.4x10^{-4}$ | $2x10^{-2}$ | $1.5x10^{-2}$ | $9.6x10^{-3}$ |
| Layer 2 – Upper shellbed | $2.1x10^{-4}$ | $7.3x10^{-4}$ | $3.65x10^{-4}$ | $2x10^{-2}$ | $4x10^{-4}$ | $3x10^{-4}$ |
| Layer 3 - Sand | Assume same as Layer 1 | | | Assume same as Layer 1 | | |
| Layer 4 – Lower shellbed | $1.3x10^{-4}$ | $7.3x10^{-4}$ | $4.4x10^{-4}$ | $3x10^{-4}$ | $4.4x10^{-3}$ | $1.6x10^{-3}$ |

### 2.3.1 Perched Aquifers and Progressive Confinement

There is anecdotal evidence of localised perched water within the wetlands and lakes in the area. For example, Lake Waiparera, located near the centre of the study area has an average lake stage of 33.8 mAMSL, yet the groundwater level estimated from an adjacent bore is around 7 mAMSL.

Before the intervention of man, lake and wetland complexes that formed in dune swales were self-accentuating over time. As fine sediment was washed into the swale with stormwater runoff, bed permeability progressively decreased due to clogging, which led to widening and deepening of the wetland or lake. As this progressed, acid conditions in the wetland environment led to dissolution of metals and as the sediment substrate conditions shifted from aerobic to anaerobic (or reducing conditions) and pH became more neutral, subsequent precipitation of the dissolved metals occurred as metal hydroxides, particularly iron hydroxide. Iron hydroxide is the primary constituent of iron humus pan or iron pan, which is the main factor (along with peat and silt deposits) in restricting vertical drainage in the Aupouri aquifer.

The aquifer system is unconfined at the surface but behaves in a manner that suggests a progressive degree of confinement with depth (leaky confinement). There is no well-defined regionally extensive confining layer but there are numerous low-permeability layers (e.g. iron pan, brown (organic) sand, silt, peat) that vary in depth and thickness, which over multiple occurrences collectively provide a degree of confinement that lends to the development of vertical pressure gradients, as discussed in **Section 2.6**.

Data collected from shallow and deep monitoring bores shows strong evidence for confinement throughout the model area. The groundwater elevations measured in shallow monitoring bores are substantially higher than the deeper monitoring bores at Sweetwater Farms in the southern portion of the model, Valic Orchards in the middle, and at the Browne and Waterfront monitoring locations in the north portion of the model area. It is likely that this is due to multiple low permeability paleosols (buried iron pans), deeply buried by successive accumulations of sand (Hicks, et. al., 2001).

## 2.4 Recharge

The proportion of rainfall that infiltrates the soils and ultimately recharges the groundwater system is relatively large, due to the high infiltration capacity of the sandy soils.

The model used in the Aupouri Aquifer Review by Lincoln Agritech (2015) suggested an annual recharge rate of 540 mm for the dune sand beneath Aupouri Forest, which accounts for 43% of annual rainfall. In other groundwater studies for the region, the percentage of rainfall recharging the dune sands ranged from 10.4% to 43.7%, while for the floodplains the recharge range was 4.2% to 12.0% of annual rainfall (HydroGeo Solutions, 2000; SKM, 2007a; SKM, 2007b).

Climate data obtained from VCSN and select gauging stations within the model area was processed through the Soil Moisture Water Balance Model (SMWBM) to generate the groundwater recharge data set to be used for model input. For the purpose of assessing recharge, FSL soil classifications are used to divide the model area into four primary recharge zones based on permeability. The zones are coastal sand, weathered sand, plains, and peat/wetlands (**Figure 3**).

Variation in rainfall and PET across the model area was accounted for by defining four regions along the north-south axis of the model and assigning climate data from an appropriate reference location for each region. The regions, included in **Figure 3**, were referred to as North, Motutangi, Waiharara-Paparore, and South. The recharge zones were then used to determine parameter inputs for SMWBM and generate daily recharge estimates based on the distribution of rainfall across the model area as defined by the climate regions described above. Further details on the process of generating the groundwater recharge data set for use in the model are provided in **Appendix B**.

This assessment resulted in 43% of mean annual rainfall applied as recharge in the coastal sand zone, 38% for the weathered sand zones, 26% for the plains in the southern portion of the model and 10% for the peat/wetlands zones. The work of WWA (2017) has been adopted in this study and is summarised in **Table 2**.

Figure 3. Recharge zones. (See A3 attachment at rear).

Table 2. The average annual water mass balance for each recharge zone from the SMWBM.

| Recharge Zone | Groundwater Recharge | Evapo-transpiration | Runoff | Description |
|---|---|---|---|---|
| Coastal sand zone | 43% | 48% | 9% | Loose sand, high infiltration capacity, low surface runoff |
| Weathered sand zone | 38% | 49% | 13% | Relatively more compacted sand, high infiltration capacity, reduced surface runoff |
| Plains zone | 26% | 54% | 20% | Moderate infiltration capacity, medium soil moisture storage, moderate surface runoff |
| Wetlands/Estuary zone | 10% | 60% | 29% | High peat content, low infiltration capacity, medium soil moisture storage, high surface runoff |

## 2.5 Drainage

In the lower-lying farmland area, there is a man-made drainage network that typically connects to short fetch streams that discharge to the coast. The drains were installed to lower the shallow groundwater table to promote more manageable farming conditions (**Figure 4**).

Figure 4. Drainage map. (See A3 attachment at rear).

## 2.6 Groundwater Level Data

There are 49 reliable monitoring piezometers located within the model area. These can be grouped into three generalized areas which are identified in **Figure 5** as the northern, central, and southern piezometer groups. Many of the piezometers have a nested configuration where up to 4 piezometers are located together with screened intervals at different depths to simultaneously monitor groundwater levels across a vertical profile. The majority of monitoring piezometers used for model calibration are maintained by the NRC, however some piezometers are privately managed.

The northern piezometer group includes five multi-level piezometers constructed by the Northland Catchment Commission in the 1980s and two single piezometers that are currently maintained for groundwater monitoring purposes in the Houhora area by the Northland Regional Council, collectively defined as the Hukatere piezometer transect.

**Figure 6** shows a cross-section of bore depths and static water levels in multi-level piezometers along the Hukatere transect (not-to-scale). The groundwater gradient shown from each piezometer nest is governed by the hydrogeological position of the piezometer on the landscape, i.e. within the recharge or discharge zone. For piezometers that are close to the groundwater divide (Browne piezometer) the observed vertical downward gradient indicates the occurrence of recharge from the surface to the deep aquifers. The piezometers near the coast at the waterfront showed an upward flow potential, indicating groundwater discharge to the sea.

The nested piezometers Burnage 1, 2 and 3 all consistently show similar groundwater levels. It likely that this is due to leakage within the piezometers at this location, thus, these three piezometers were excluded in the model calibration.

The central group of monitoring piezometers, shown in **Figure 7**, includes NRC monitoring bores at Ogle Drive and Paparore. The latter of these has four nested monitoring piezometers ranging in depth from 18 to 75 mBGL. There are four monitoring locations on the Valic Avocado Orchard. Each location features a monitoring bore drilled into the deep aquifer at a similar depth to the nearby production bore and an additional monitoring bore in the shallow aquifer. Vertical hydraulic gradients between the shallow and deep aquifer at the Valic Avocado Orchard range from 6 to 11 meters. By contrast the monitoring piezometers at Paparore measure a minimal vertical hydraulic gradient between the two aquifers, with a slightly greater head measured at the deeper bores relative to the shallow ones.

The southern group of monitoring piezometers are shown in **Figure 8**. The majority of these bores are managed by Sweetwater Farms, where there are 5 pairs of deep and shallow monitoring bores, as well as several additional bores where only one depth is monitored. There are also NRC operated bores at Lake Heather and several independently operated bores where water level data is available, specifically, at Vinac, Waipapa, and Welch.

A vertical downward gradient of groundwater head is evident at Sweetwater Monitoring Wells #1, #3, #4, and #5, though in the case of #4 it is likely that the shallow piezometer is measuring a perched water table based on the groundwater elevation being higher than what is measured in other shallow monitoring wells located further inland. Sweetwater Monitoring Well #2 is the only case where groundwater level measurements indicate an upward groundwater gradient.

Figure 5. Location of monitoring piezometers. (See A3 attachment at rear).

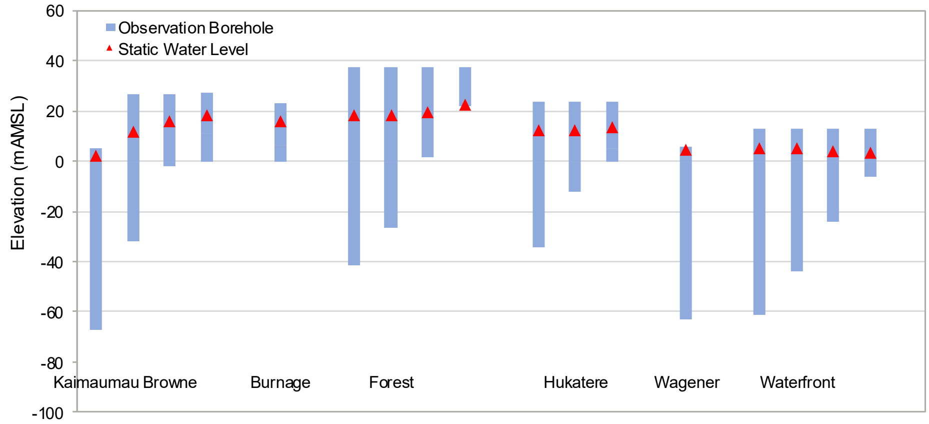


Figure 6. Mean groundwater levels of monitoring piezometers in the northern portion of the model area

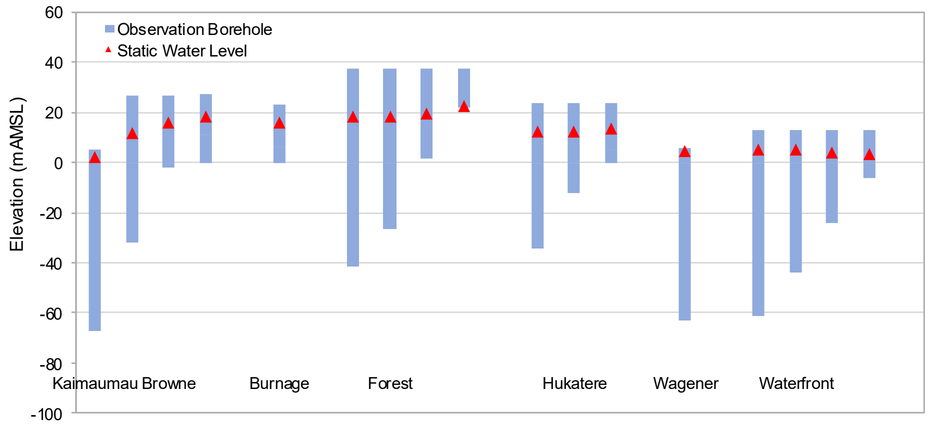


Figure 7. Mean groundwater levels of monitoring piezometers in the central portion of the model area

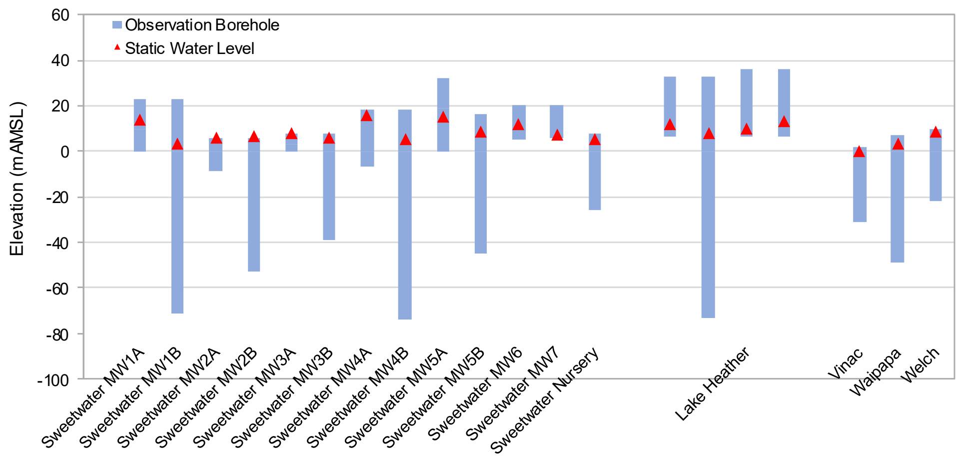


Figure 8. Mean groundwater levels of monitoring piezometers in the southern portion of the model area

## 2.7 Groundwater Abstraction

**Figure 9** shows the location of existing and recently proposed groundwater abstraction consents.

The current level of annual groundwater abstraction from the Aupouri aquifer is 4.79x$10^6$ $m^3$/year distributed among 58 consents that are currently being exercised. Some of these consents are exercised through the operation of multiple bores.

An additional 3.13x$10^6$ $m^3$/year have been granted but are not currently being exercised. The unexercised consents include the newly granted groundwater takes for the 17 irrigators collectively known as the Motutangi Water Users Group, a portion of the water that has been allocated to Sweetwater Farms, and the Far North District Council groundwater take for Kaitaia.

There are also 28 expired groundwater take consents within the model area, totalling 8.53x $10^6$ $m^3$/year of abstraction. These takes were not included in the total amount of currently allocated groundwater, but they were used for developing a historical dataset. **Appendix C** provides consented and proposed groundwater takes corresponding to the locations shown in **Figure 9A** through **Figure** 9**C**.

Figure 9A. Location of existing and proposed groundwater take bores in northern portion of model. (See A3 attachment at rear).

Figure 9B. Location of existing and proposed groundwater take bores in central portion of model. (See A3 attachment at rear).

Figure 9C. Location of existing and proposed groundwater take bores in southern portion of model. (See A3 attachment at rear).

### 2.7.1 Actual Use Dataset

A historical actual use dataset is required to more accurately calibrate a groundwater model and to thereafter use the model to simulate the effects of groundwater extraction on the aquifer and surface water resources.

The SMWBM Irrigation Module was used to develop an estimate of historical actual use. The exercise combined typical irrigation scheduling (Oct - Apr) and the commencement dates that the consents were granted, along with an allowance for orchard development and tree growth rates to maximum water requirement. Details and results of the development of the actual use dataset are provided in **Appendix D**.

A complete dataset of historic groundwater use within the model area was not available, therefore a conservative estimate of groundwater use was generated by assuming that all active consents were available from the beginning of the simulation period with the exception of the two Sweetwater Farms production bores that were known to have initiated operation in 2015 and 2017, respectively and the Valic 1 through 3 production bores where pumping operations are known to have stated in 2007. **Figure 10** shows the total annual volume of simulated actual use as applied in the model.

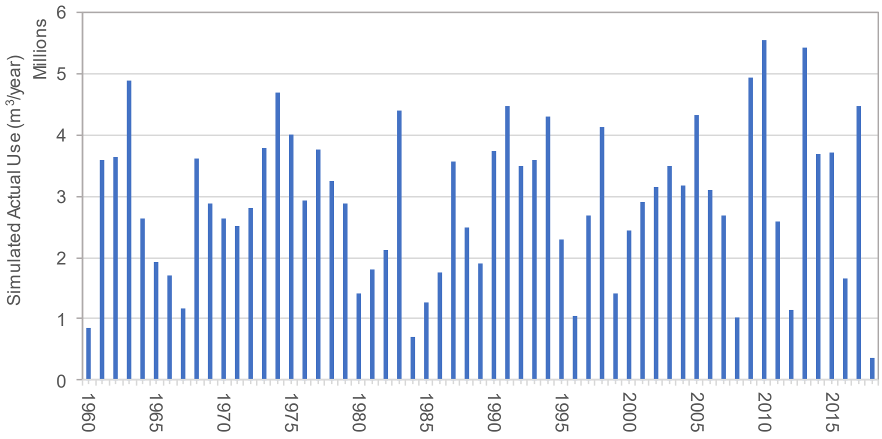


Figure 10. Simulated groundwater extraction (m³/year; partial groundwater use in 2018 due to the end of the model simulation).

# 3. Model Configuration

The MODFLOW Unstructured Grid (MODFLOW-USG) developed by the United States Geological Survey (USGS) was utilised within the GMS10.2 modelling platform to construct the groundwater flow model in this project. The unstructured discretisation of the model domain provides the capacity of fitting irregular boundaries into the model and increasing the resolution in the areas of maximum interest and decreasing resolution in other areas, hence increasing the efficiency in model computation compared to the equivalent regular MODFLOW grid.

## 3.1 Model Domain

The model was constructed based on six layers, with a total of 147,252 active Voronoi cells (or polygons), and covers an area of 535 km$^2$. Grid spacing ranges from 40 m at the highest resolution, centred around large groundwater extraction points, to 1,000 m in the northwest portion of the model area where high resolution is unnecessary. This spatially varying discretisation approach reduces model computational time while maintaining better model resolution at the points of interest (**Figure 11**).

Figure 11. Plan view of unstructured model grid discretisation (See A3 attachment at rear).

The boundary conditions included in the model are constant head, general head, drain, and no-flow boundaries.

### 3.1.1 Constant Head Boundaries

The constant head boundary was assigned an elevation of 0 mAMSL along the eastern and western coastlines in Layer 1 of the model to represent the mean hydraulic head of the ocean at these locations.

### 3.1.2 General Head Boundaries

A general head boundary (GHB) is typically used to simulate the flow interaction between groundwater and external water sources to the model domain.

There are 16 lakes within the model area that are large enough to occupy the majority of a model cell and were therefore incorporated into the model. It was determined that these lakes occur due to buried hard pans causing localized perching without a direct connection to the regional water table. The conclusion that there is disconnection between surface lakes and regional groundwater is consistent with the findings of other studies such as Lincoln Agritech (2015) and WWA (2017). A GHB was assigned to cells primarily occupied by lakes, to simulate lake water seeping to the underlying groundwater system, with consideration of the impedance provided by the lower-permeability lake bed sediments and/or iron pan. The head stage assigned for the GHB for each lake was determined by extracting the average elevation for each lake based on the model area DEM.

Lake Waiparera, located in the middle the model domain is the largest lake in the model domain. It was observed to have an average lake stage of 33.8 mAMSL while the groundwater level, estimated from the adjacent bore, was around 7 mAMSL, indicating that Lake Waiparera is perched above the regional groundwater system. This is also consistent with the conclusion made in the Aupouri Aquifer Review Report that the main aquifer is situated well below the surface of Lake Waiparera (Lincoln Agritech, 2015).

Similar findings can be demonstrated at Lake Heather where the mean surface elevation of the lake was determined to be 32.1 mAMSL whereas shallow monitoring piezometers located near the lake show groundwater elevations of 12.0 and 13.1 mAMSL.

The cells along the coastline from Layer 2 to 6 were also assigned with GHBs. The head values for all the cells were assigned as 0 mAMSL and the conductance value of each layer decreases with depth. This is to reflect the progressively increasing disconnection of the groundwater with the free water surface of the ocean (i.e. the impedance of flow to the ocean floor increases with depth) and also the resistance of higher-density seawater offshore. It was estimated based on the model calibration that the cells along the west coast boundary had approximately one order of magnitude lower conductance than the cells along the east coast boundary.

### 3.1.3 No-Flow Boundaries

The AAGWM was designed to encompass the entire Aupouri aquifer therefore no-flow boundaries were assigned to cells located on the northern and southern boundaries of the model domain representing the margin of the aquifer. In the north groundwater is expected to predominantly flow downgradient toward the south and laterally to the coasts while in the south bedrock outcroppings form a boundary to groundwater flow. The base of the model was also assigned a no-flow boundary on the basis that the significantly lower permeability of the basement rocks has negligible bearing on the overall flow budget of the aquifer system above.

### 3.1.4 Drain Boundaries

Drain boundaries were assigned in the model to simulate the groundwater discharged to the major surface drains, and to simulate the estuary that occurs along the east coast portion of the model area. The drain bed elevations were derived from the Digital Elevation Model (DEM), with a nominal depth assignment depending on locality as follows:

- Drains in farmland – DEM minus 3 m;
- Drains in estuary – DEM minus 0.5 m;
- Drains in wetland outside of estuary – DEM minus 3 m.

The conductance value of the drains was set relatively high to reflect limited impedance to water removal (or drain functionality), to account for the significant water drainage in the farmland area and flow of water over the surface in the wetland.

### 3.1.5 Well Boundaries

Well points were used to represent the groundwater extraction from within the model. The corresponding model cells were assigned with negative pumping rates to represent the groundwater extraction from the model.

## 3.2 Simulation Package

### 3.2.1 Sparse Matrix Solver

The Sparse Matrix Solver (SMS) package was utilised to solve linear and non-linear equations. A maximum head change of 0.01 m between iterations was set as the model convergence criteria. Default values were used for the maximum number of iterations for linear and non-linear equations.

### 3.2.2 Ghost Node Correction Package

MODFLOW-USG is built on the control volume finite difference formulation, which enables the model cell to be connected to an arbitrary number of adjacent cells (Panday et al., 2013). However, this formulation will be reduced to a lower order of approximation, when the line between two connected nodes does not bisect the shared face at right angles, which will lead to errors in the simulation (Edwards, 1996). To account for this, the ghost node correction package was utilised to improve the simulation results by adding higher order correction terms in the matrix solver. Ghost nodes are implicitly built into the simulation through the interpolation factors. The simulated head is systematically corrected through the ghost nodes to achieve a correct solution.

## 3.3 Model Layer Configuration

### 3.3.1 Layer Geology

The model comprises six layers that are used to represent the varying geology located in the area. The geological units assigned to each layer of the numerical model are shown in **Table 3**.

Table 3. Geological units in the model conceptualisation.

| Model Layer | Stratigraphic Layer | Name | Description | Locality |
|---|---|---|---|---|
| 1-3 | 1 | Coastal sand | Loose coastal sand, highly permeable | Western and eastern coastal strips. |
| | 1 | Weathered sand | Weathered dune sand, moderately compacted | Inland hilly or rolling country areas. |
| | 1 | Wetland/Estuary | Peaty and clayey sediments, low permeability | Low lying region along east coast including Kaimaumau wetland. Only applied for Model layer 1. |
| | 1 | Plains | Peaty and clayey sediments with some sand, low-moderate permeability | Inland low-lying plains areas in southern region of model. Only applied for Model layer 1. |
| 4 | 2 | Shellbed | Sand presented with shells, highly permeable | Throughout model, albeit thickness varies. |
| 5 | 3 | Fine sand | Old sand deposits, fine sand, moderately permeable | |
| 6 | 4 | Shellbed | Sand presented with more shells, highly permeable | |

Model Layers 1-3 are used to represent a complex stratigraphic unit comprising alternating sands, silt, peat, clay and iron pans in a bulk sense (not discretely). The sub-division of this stratigraphic unit into layers is complex because layering is varied both horizontally and vertically. For modelling purposes, horizontally continuous and vertically discrete layers are required to enable anisotropy to be incorporated in the model calibration process; hence the base of model Layer 1 was defined as an elevation of -2.0 mAMSL, while the base of model Layer 2 was set at 22 m above the base of model Layer 3. Based on the 10 m vertical hydraulic gradient observed in the monitoring data at Valic-2 from the Valic-2 shallow and deep piezometers, it is likely that there is a localised zone of low permeability in the subsurface in this region. This was incorporated into the model as a limited region of low conductivity relative to the surrounding material.

All model layer bases other than model Layer 1 and 2 conform to stratigraphic interpolations as discussed in the following section.

### 3.3.2 Layer Elevations

The top and bottom elevation for the geological unit contacts were determined through a process of reviewing 198 bore logs at locations within the model area. The majority of the bore logs were obtained by request through the NRC while some additional bore logs were provided directly through the bore owners. Each bore log was reviewed to characterize the primary material types within the context of the conceptual geological configuration incorporated into the model. The bottom elevations for each unit were then interpolated using the Kriging geospatial method to generate a digital elevation surface.

The geometry of the basement rocks has been recognised through interpolation of the basal contact from the available bore logs in the area and was considered to be the lower model boundary where interfaced with the lower shellbed. During interpolation, rules were applied so that geological layers did not overlap, and the surface is stratigraphically continuous.

**Figure 12** through **Figure 15** show interpolated elevation contours used for the model layer interfaces and basement elevation (i.e. the model bottom).

Figure 12. Bottom elevation of sand and peat layers (model Layers 1-3 base). (See A3 attachment at rear).

Figure 13. Bottom elevation of upper shellbed (model Layer 4 base). (See A3 attachment at rear).

Figure 14. Bottom elevation of compact sand layers (model Layer 5 base). (See A3 attachment at rear).

Figure 15. Basement rock elevation contours (model Layer 6 base). (See A3 attachment at rear).

Geological cross-sections were developed from selected transects through the kriged surfaces in north-south (N-S) and west-east (E-W) directions to demonstrate the relative thickness of each geological unit. Transects are identified by the section of the model where they are located and are shown in **Figure 16** while the cross-sections themselves are shown in **Figure 17** to **Figure 24**. The constructed model grid based on the interpolated layer elevations is shown in **Figure 25**.

Figure 16. Hydrogeological cross section locations. (See A3 attachment at rear).

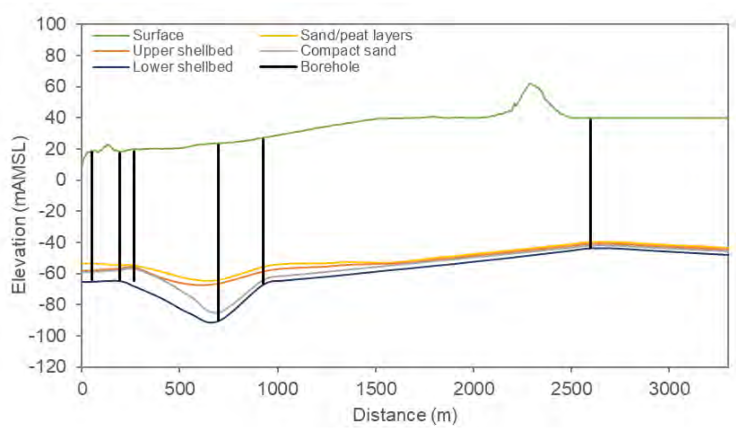


Figure 17. Interpolated cross-section **A to A' showing** bore locations (refer to Figure 16 for location).

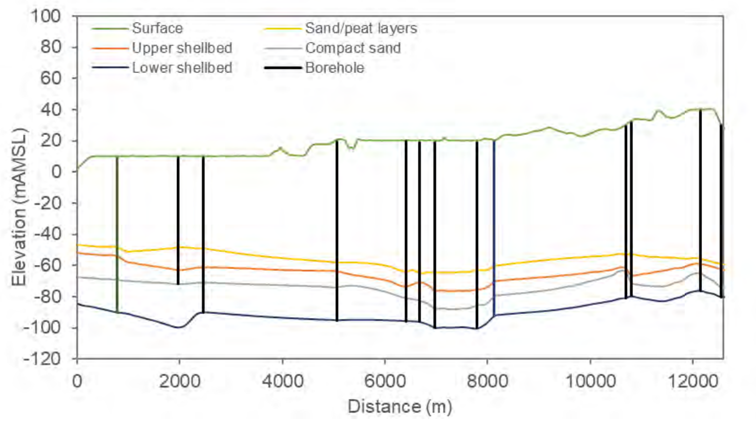


Figure 18. Interpolated cross-**section B to B' showing bore locations** (refer to Figure 16 for location).

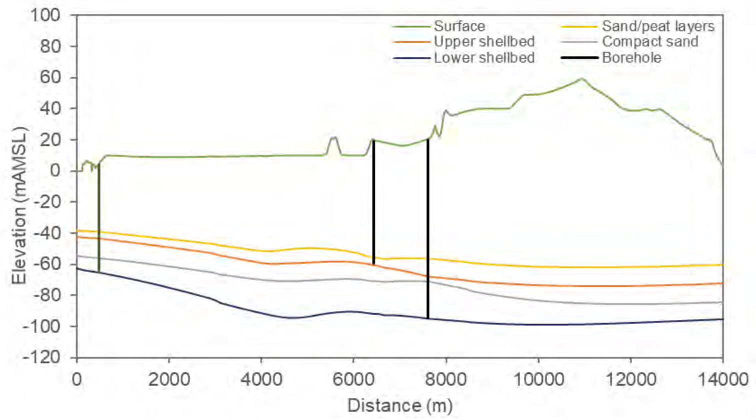


Figure 19. Interpolated cross-**section C to C' showing bore locations** (refer to Figure 16 for location).

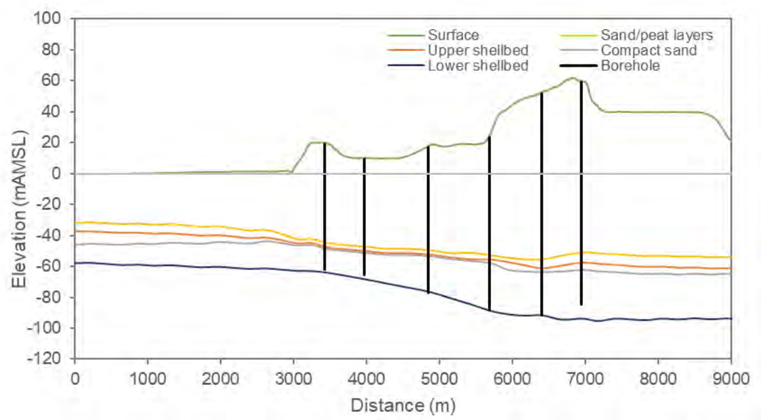


Figure 20. Interpolated cross-**section D to D' showing bore locations** (refer to Figure 16 for location).

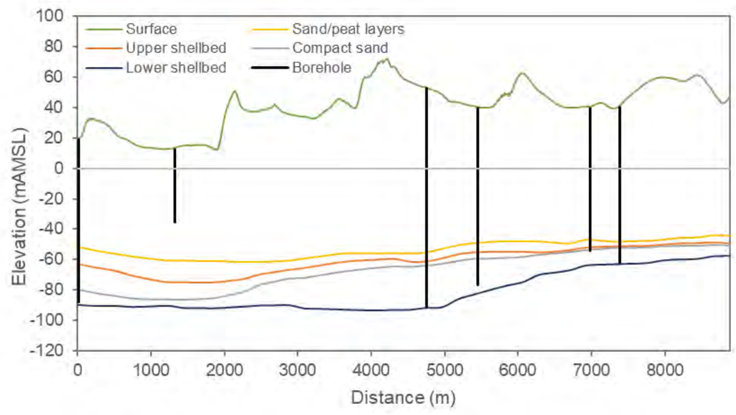


Figure 21. Interpolated cross-section E to E' **showing bore locations** (refer to Figure 16 for location).

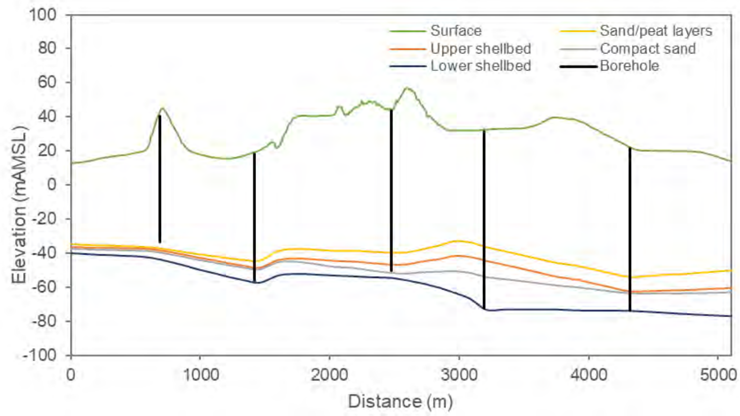


Figure 22. Interpolated cross-section F to F' **showing bore locations** (refer to Figure 16 for location).

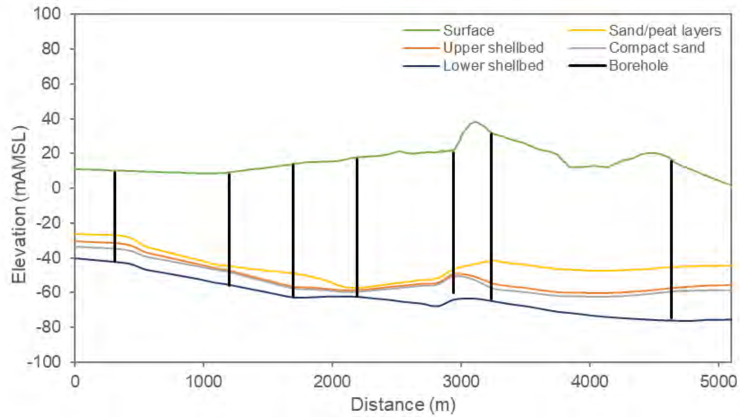


Figure 23. Interpolated cross-section G to G' **showing bore locations** (refer to Figure 16 for location).

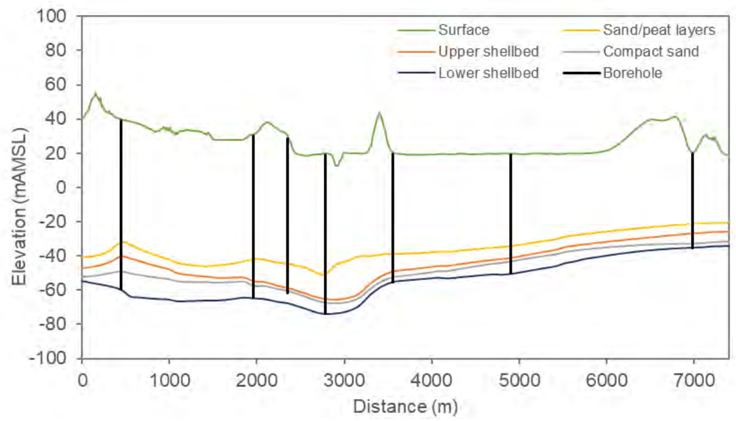


Figure 24. Interpolated cross-**section H to H' showing bore locations (refer to Figur**e 16 for location).

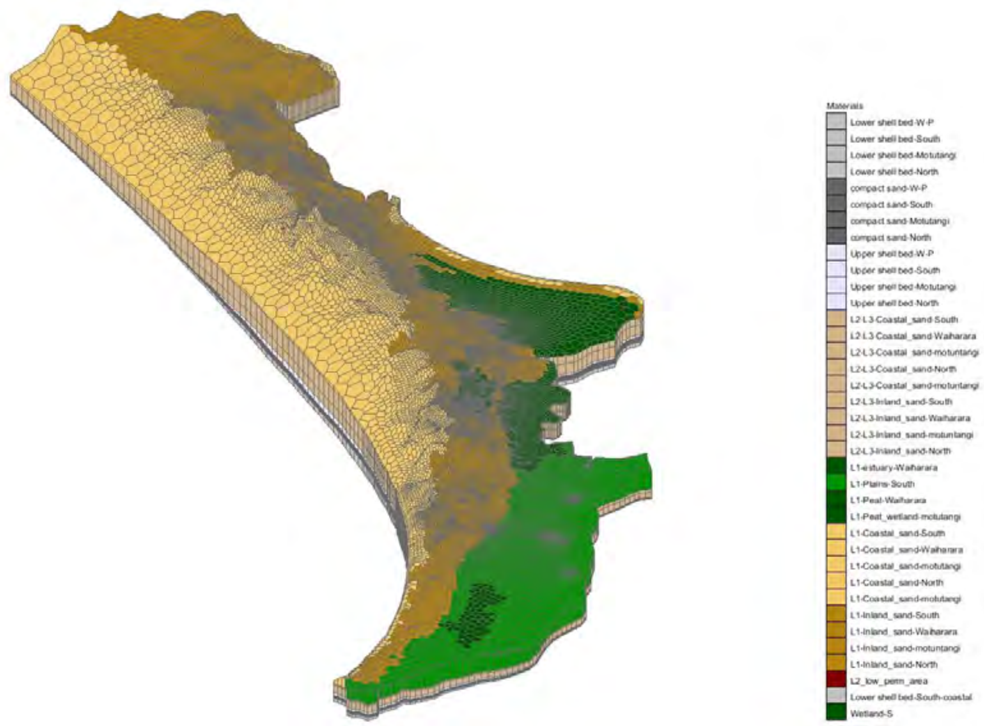


Figure 25. MODFLOW grid with vertical magnification of 25.

# 4. Model Calibration

The model calibration was conducted by manually changing the model hydraulic parameters to achieve an acceptable fit to measured groundwater levels. Groundwater recharge was not considered a calibration parameter.

## 4.1 Observation Points

The piezometers used for calibration of the model are shown in **Figure 5** and the key properties of the piezometers relevant to model calibration are summarised in **Error! Reference source not found.**. The piezometers include nested piezometer configurations comprising adjacent standpipes installed to different depths or aquifer levels and standalone piezometers measuring a single depth. Vertical pressure gradients are evident where there are concurrent measurements from nested piezometers measuring different depths at a single location. Achieving a simulated vertical pressure gradient requires multiple layers with vertical anisotropy to be incorporated in the model (as discussed in **Section 2.6**). To achieve this, a finer vertical discretisation of the model was required, and this was a key driver for splitting stratigraphic Layer 1 into three model layers as described in **Section 3.3**. The discrete layers enabled vertical anisotropy to be considered in model calibration as a bulk property within each layer while providing flexibility to vary anisotropy vertically to account for the heterogeneous nature of the materials.

Table 4. Key specifications of the observation bores used for model calibration.

| Model Region | Site | Piezometer Description | Mean groundwater level (mAMSL) | Standard deviation (m) | Bore depth (m) | Model Layer |
|---|---|---|---|---|---|---|
| Hukatere Transect | Waterfront | NRC shallow monitoring bore | 3.46 | 0.36 | 19.0 | 2 |
| | | NRC middle monitoring bore | 3.99 | 0.36 | 37.0 | 2 |
| | | NRC deep monitoring bore | 5.33 | 0.28 | 57.0 | 3 |
| | | NRC deep monitoring bore | 5.30 | 0.29 | 74.0 | 4 |
| | Hukatere | NRC shallow monitoring bore | 13.79 | 1.26 | 19.0 | 1 |
| | | NRC middle monitoring bore | 12.68 | 1.15 | 36.0 | 2 |
| | | NRC deep monitoring bore | 12.26 | 1.11 | 58.0 | 2 |
| | Forest | NRC shallow monitoring bore | 20.45 | 1.07 | 16.0 | 1 |
| | | NRC middle monitoring bore | 19.47 | 1.31 | 36.0 | 1 |
| | | NRC deep monitoring bore | 18.20 | 1.17 | 64.0 | 2 |
| | | NRC deep monitoring bore | 18.18 | 1.17 | 79.0 | 3 |
| | Burnage | NRC shallow monitoring bore | 16.14 | 0.71 | 17.0 | 1 |
| | Browne | NRC shallow monitoring bore | 18.67 | 0.93 | 16.0 | 1 |
| | | NRC shallow monitoring bore | 15.81 | 0.82 | 29.0 | 1 |
| | | NRC deep monitoring bore | 11.53 | 0.78 | 59.0 | 2 |
| | Wagener Golf Club | Deep monitoring bore | 4.48 | 0.28 | 69.0 | 4 |
| | Fishing Club at Houhora | Deep monitoring bore | 3.43 | 0.61 | 78.0 | 5 |

| Model Region | Site | Piezometer Description | Mean groundwater level (mAMSL) | Standard deviation (m) | Bore depth (m) | Model Layer |
|---|---|---|---|---|---|---|
| Waiharara-Paparore Region | Kaimaumau Deep | NRC | 2.44 | 0.82 | 72.0 | 6 |
| | Ogle Drive | NRC Monitoring Bore | 14.90 | 0.32 | 68.0 | 3 |
| | Paparore | NRC deep monitoring bore | 6.88 | 0.66 | 75.0 | 6 |
| | | NRC deep monitoring bore | 6.88 | 0.63 | 65.0 | 4 |
| | | NRC middle monitoring bore | 6.46 | 0.26 | 35.0 | 2 |
| | | NRC shallow monitoring bore | 6.42 | 0.27 | 18.0 | 1 |
| | Valic-1 | Shallow Monitoring Bore | 21.74 | 0.47 | 17.0 | 1 |
| | | Deep monitoring bore | 11.65 | 0.83 | 103.0 | 6 |
| | | Production Bore | 11.41 | 0.83 | 103.0 | 6 |
| | Valic-2 | Shallow Monitoring Bore | 22.88 | 0.77 | 55.0 | 1 |
| | | Deep monitoring bore | 12.24 | 1.00 | 121.0 | 6 |
| | | Production Bore | 12.06 | 0.85 | 121.0 | 6 |
| | Valic-3 | Shallow Monitoring Bore | 20.99 | 0.76 | 45.0 | 1 |
| | | Deep monitoring bore | 11.28 | 1.94 | 124.0 | 6 |
| | | Production Bore | 11.32 | 2.23 | 124.0 | 6 |
| | Valic-4 | Shallow Monitoring Bore | 20.99 | 0.76 | 45.0 | 1 |
| | | Deep monitoring bore | 11.28 | 1.94 | 124.0 | 6 |
| | | Production Bore | 10.75 | 0.55 | 93.0 | 6 |
| Sweetwater Farms Monitoring Wells | Sweetwater MW1 | Shallow Monitoring Bore | 13.84 | 0.48 | 13.3 | 1 |
| | | Deep monitoring bore | 2.83 | 2.13 | 94.0 | 6 |
| | Sweetwater MW2 | Shallow Monitoring Bore | 5.82 | 0.19 | 14.5 | 2 |
| | | Deep monitoring bore | 6.35 | 0.27 | 59.0 | 6 |
| | Sweetwater MW3 | Shallow Monitoring Bore | 7.61 | 0.29 | 5.0 | 1 |
| | | Deep monitoring bore | 5.83 | 0.30 | 47.0 | 6 |
| | Sweetwater MW4 | Shallow Monitoring Bore | 15.56 | 0.50 | 25.0 | 2 |
| | | Deep monitoring bore | 4.98 | 0.22 | 92.0 | 6 |
| | Sweetwater MW5 | Shallow Monitoring Bore | 15.09 | 0.92 | 6.0 | 1 |
| | | Deep monitoring bore | 8.67 | 0.74 | 61.0 | 6 |
| | Sweetwater MW6 | Shallow Monitoring Bore | 11.88 | 0.81 | 15.0 | 1 |
| | Sweetwater MW7 | Shallow Monitoring Bore | 15.92 | NA | 7.0 | 1 |
| | Sweetwater Nursery | Monitoring bore | 10.50 | 0.43 | 33.8 | 3 |
| Lake Heather Monitoring Bores | Lake Heather Piezometer 1 | NRC shallow monitoring bore | 11.97 | 0.93 | 26.0 | 1 |
| | | NRC deep monitoring bore | 8.04 | 0.66 | 105.5 | 6 |
| | Lake Heather Piezometer 2 | NRC shallow monitoring bore | 9.56 | 0.94 | 29.5 | 1 |
| | Lake Heather Piezometer 3 | NRC shallow monitoring bore | 13.11 | 0.74 | 29.0 | 1 |

| Model Region | Site | Piezometer Description | Mean groundwater level (mAMSL) | Standard deviation (m) | Bore depth (m) | Model Layer |
|---|---|---|---|---|---|---|
| Private Bores in Southern Aupouri Aquifer | Vinac | Private bore | 0.04 | 0.75 | 33.0 | 4 |
| | Waipapa | Private bore | 2.93 | 0.14 | 56.0 | 4 |
| | Matich | Private bore | 4.73 | 0.18 | Unknown | 1 |
| | Welch | Private bore | 8.12 | 0.39 | 31.7 | 3 |
| | Shanks | Private bore | 7.20 | 0.39 | Unknown | 1 |

## 4.2 Steady-State Calibration

A steady-state model was developed and calibrated to validate the conceptualisation of the groundwater flow model. The objective of the calibration was to obtain approximate values of the model parameters, and to obtain initial heads for transient model simulation. An automated parameter estimation tool, PEST, was used to calibrate hydraulic conductivity and vertical anisotropy of materials for each of the 6 model layers with constraints based on previous modelling studies for the region and literature values.

For calibration purposes material zones within the model domain were defined vertically based on the model layers described in **Section 3.3** and divided horizontally into four sections along a north-south axis. These zones are shown in **Figure 26** and referred to herein, from north to south as North, Motutangi, Waiharara-Paparore, and South.

Figure 26. Aupouri Aquifer Groundwater Model parameter calibration zones (See A3 attachment at rear).

These divisions were made to enable a model calibration that reflects the fact that the material is heterogeneous and therefore hydraulic characteristics are spatially variable within a given material. The four zones that were defined for the north-south axis were based on geographic areas where groundwater takes are concentrated or where landscape variability was considered likely to indicate variation in hydrogeological characteristics.

Through this method the best possible calibration for the data set was achieved for the setup while ensuring that calibrated parameters were reasonable for the given material types.

The average water levels from 56 piezometers registered on the NRC bore database were used as the calibration targets. The simulated head is plotted against the observations (**Figure 27**). The steady-state simulation has a mean head residual of -0.42 m (indicating a net over-simulation of groundwater head), and root mean square error (RMSE) of 2.1 m, which is approximately 7.9% of the range of observations. The RMSE has been affected by the following observations:

- ***Paparore (Middle and Shallow Bores)*** - Simulated vertical hydraulic gradient is greater than what has been observed indicating a local variation in stratigraphy not captured by the model.
- ***Browne-1*** - Simulated head was greater than observed data, however given that the 2 shallowest of the nested piezometers at this location both correspond to model layer 1, yet have a difference of 4.3 m in mean head it would be impossible to match both piezometers given the construct of the model (i.e. groundwater head will be hydrostatic within a single layer). The match for simulated head in the deeper of the two piezometers, Browne-2 is within 1.3 m of the mean measured value.

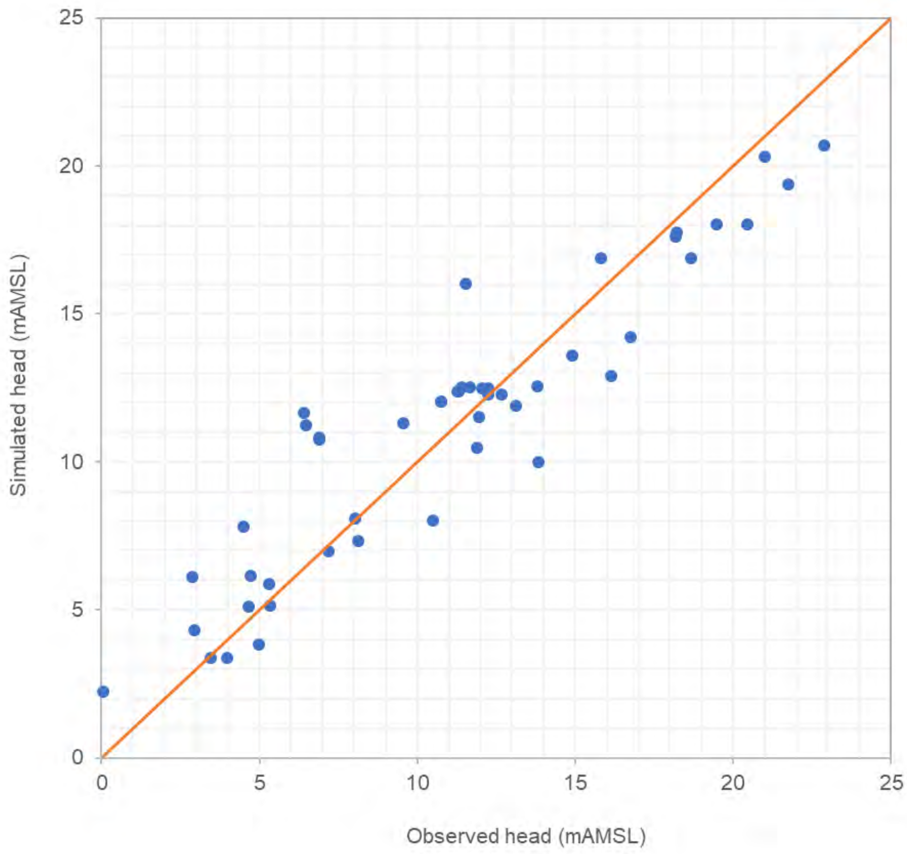


Figure 27. Simulated head versus observed head.

## 4.3 Transient Calibration

The calibrated parameters from the steady state PEST simulation were used as a starting point for calibrating the transient model. Targeted adjustments were made to hydraulic conductivity, vertical anisotropy, drain elevation, and the conductivity of subsurface boundaries (only on the west coast).

The model was simulated approximately 75 times to obtain a satisfactory calibration. Each transient simulation takes 30 minutes to run, and post processing of results takes 3 minutes, hence a cycle time of approximately 33 minutes is needed for each model simulation. This cycle time enabled a significant number of calibration and sensitivity assessment runs to be undertaken.

After each run, simulated heads from the relevant model layer and cell were extracted and processed with Python code that automatically developed hydrographs and calculated RMSE for each gauge individually, which permitted rapid comparison of simulated versus measured data.

The transient calibration setup is described in the following sections.

### 4.3.1 Stress Periods and Time Steps

The model was simulated in transient mode for 58.6 years from 1/01/1960 to 31/07/2018. The simulation was subdivided into 371 stress periods, where imposed stresses (e.g. recharge and pumping) remain constant. The number of stress periods was selected on the basis of i) temporal variation of the transient dataset values; and ii) computational time. The resulting stress period lengths ranged from 13 to 185 days. Stress periods were locked on 1 October and 30 April in each year for the start and end of the irrigation season, respectively, to ensure the irrigation demands were distributed to the correct timeframe.

Each stress period consisted of five time-steps, with head and flow volume in each model cell evaluated at the end of each time step.

### 4.3.2 Groundwater Pumping

The estimated historical use dataset described in **Section 2.7.1** was implemented in the calibration simulations.

### 4.3.3 Initial Conditions

The transient model used the steady-state model heads as the starting condition. During the transient calibration process, the starting heads were re-set periodically as parameters were updated. This enabled the starting condition to better reflect the dynamic head distribution within the model under the imposed set of stresses and resulted in minimisation of rapid fluctuations in simulated levels and flows at the start of the simulation (i.e. increased stability).

### 4.3.4 Model Parameters

The model was calibrated by adjusting parameters for materials both horizontally and vertically to best simulate groundwater elevations measured at observation bores. The calibrated model parameters are shown in **Table 5**. The calibrated model parameters, where applicable, are consistent with calibrated model parameters used in previous modelling (WWA, 2017; WWA, 2018).

The calibrated model hydraulic conductivity for the upper shellbed aquifer ranges from $2.2 \times 10^{-4}$ m/s in the Waiharara-Paparore region to $4.9 \times 10^{-4}$ m/s in the Motutangi region. In the lower shellbed aquifer conductivity ranges from $3.1 \times 10^{-4}$ m/s in the Motutangi region to $5.8 \times 10^{-4}$ m/s in the South region. As shown in **Table 1,** these values are within the range of horizontal hydraulic conductivity measured and modelled in the past for both the upper and lower shellbed aquifers (Layer 2 and 4). Similarly, for the various sand units, the calibrated model values range from $1.0 \times 10^{-5}$ m/s to $8.3 \times 10^{-5}$ m/s, which is consistent with the range in previously documented values as shown in **Table 1.** Calibrated hydraulic conductivity in the wetland, estuary and peat zones is somewhat lower in the Motutangi and Waiharara regions.

Table 5. Calibrated model parameters.

| Model Layer | Model Geological Units | Kx | | Vertical Anisotropy | Sy | Ss |
|---|---|---|---|---|---|---|
| | | (m/d) | (m/s) | (-) | (-) | (m-1) |
| Layer 1: Interbedded sand, peat, and iron pans | Coastal sand-North | 4.20 | 4.9E-05 | 8 | - | 0.30 |
| | Coastal sand-Motutangi | 4.85 | 5.6E-05 | 56 | - | 0.30 |
| | Coastal sand-Waiharara-Paparore | 2.75 | 3.2E-05 | 24 | - | 0.30 |
| | Coastal sand-South | 6.69 | 7.7E-05 | 24 | - | 0.30 |
| | Inland sand-North | 2.40 | 2.8E-05 | 16 | - | 0.25 |
| | Inland sand-Motutangi | 2.93 | 3.4E-05 | 103 | - | 0.25 |
| | Inland sand-Waiharara-Paparore | 1.65 | 1.9E-05 | 51 | - | 0.25 |
| | Inland sand-South | 0.90 | 3.5E-06 | 85 | - | 0.25 |
| | Peat wetland-Motutangi | 0.12 | 1.4E-06 | 12 | - | 0.05 |
| | Peat-Waiharara-Paparore | 0.6 | 6.9E-06 | 12 | - | 0.05 |

| Model Layer | Model Geological Units | Kx | | Vertical Anisotropy | Sy | Ss |
|---|---|---|---|---|---|---|
| | | (m/d) | (m/s) | (-) | (-) | (m-1) |
| | Estuary-Waiharara-Paparore | 1.00 | 1.2E-05 | 12 | - | 0.10 |
| | Plains-South | 5.00 | 5.8E-05 | 12 | - | 0.20 |
| Layers 2 & 3: Interbedded sand, peat, and iron pans | Coastal sand-North | 4.20 | 4.9E-05 | 8 | 5.0E-04 | - |
| | Coastal sand-Motutangi | 4.80 | 5.6E-05 | 24 | 5.0E-04 | - |
| | Coastal sand-Waiharara-Paparore | 2.55 | 3.0E-05 | 32 | 5.0E-04 | - |
| | Coastal sand-South | 12.00 | 1.4E-04 | 32 | 5.0E-04 | - |
| | Inland sand-North | 4.20 | 4.9E-05 | 8 | 5.0E-04 | - |
| | Inland sand-Motutangi | 3.36 | 3.9E-05 | 72 | 5.0E-04 | - |
| | Inland sand-Waiharara-Paparore | 2.25 | 2.6E-05 | 48 | 5.0E-04 | - |
| | Inland sand-South | 1.20 | 1.7E-05 | 50 | 5.0E-04 | - |
| Layer 4: Upper Shellbed | Upper Shellbed-North | 36.00 | 4.2E-04 | 1 | 1.1E-03 | - |
| | Upper Shellbed-Motutangi | 42.00 | 4.9E-04 | 1 | 1.1E-03 | - |
| | Upper Shellbed-Waiharara-Paparore | 19.20 | 2.2E-04 | 1 | 1.1E-03 | - |
| | Upper Shellbed-South | 30.00 | 3.5E-04 | 1 | 1.1E-03 | - |
| Layer 5: Compact Sand | Compact sand-North | 1.20 | 1.4E-05 | 48 | 1.6E-04 | - |
| | Compact sand-Motutangi | 7.20 | 8.3E-05 | 29 | 1.6E-04 | - |
| | Compact sand-Waiharara-Paparore | 0.60 | 6.9E-06 | 48 | 1.6E-04 | - |
| | Compact sand-South | 1.50 | 1.7E-05 | 72 | 1.6E-04 | - |
| Layer 6: Lower Shellbed | Lower Shellbed-North | 36.00 | 4.2E-04 | 1 | 1.1E-03 | - |
| | Lower Shellbed-Motutangi | 26.40 | 3.1E-04 | 1 | 1.1E-03 | - |
| | Lower Shellbed-Waiharara-Paparore | 42.00 | 4.9E-04 | 1 | 1.1E-03 | - |
| | Lower Shellbed-South | 50.00 | 5.8E-04 | 1 | 1.1E-03 | - |

## 4.4 Calibrated Model Output

### 4.4.1 Groundwater Levels

As previously stated in **Section 2.6**, groundwater levels recorded within 17 NRC monitoring piezometers were used to calibrate the transient groundwater model. **Appendix E** provides hydrographs and water level maps of simulated groundwater levels plotted against observed data for comparison purposes, and calibration results for each observation bore are shown in **Table 6**. The observation bores referenced in **Table 6** are the same as those described in **Section 4.1** and shown in **Figure 5**

Table 6. Model calibration results at observation bores.

| Model Region | Site | Piezometer Description | Root Mean Squared Error | Mean groundwater level (mAMSL) | Bore depth | Model Layer |
|---|---|---|---|---|---|---|
| Hukatere Transect | Waterfront | NRC shallow monitoring bore | 0.36 | 3.46 | 19.0 | 2 |
| | | NRC middle monitoring bore | 0.73 | 3.99 | 37.0 | 2 |
| | | NRC deep monitoring bore | 0.36 | 5.33 | 57.0 | 3 |
| | | NRC deep monitoring bore | 0.57 | 5.30 | 74.0 | 4 |
| | Hukatere | NRC shallow monitoring bore | 1.69 | 13.79 | 19.0 | 1 |
| | | NRC middle monitoring bore | 0.99 | 12.68 | 36.0 | 2 |
| | | NRC deep monitoring bore | 0.77 | 12.26 | 58.0 | 2 |
| | Forest | NRC shallow monitoring bore | 2.83 | 20.45 | 16.0 | 1 |
| | | NRC middle monitoring bore | 1.97 | 19.47 | 36.0 | 1 |
| | | NRC deep monitoring bore | 1.08 | 18.20 | 64.0 | 2 |
| | | NRC deep monitoring bore | 1.18 | 18.18 | 79.0 | 3 |
| | Burnage | NRC shallow monitoring bore | 3.54 | 16.14 | 17.0 | 1 |
| | Browne | NRC shallow monitoring bore | 2.18 | 18.67 | 16.0 | 1 |
| | | NRC shallow monitoring bore | 0.89 | 15.81 | 29.0 | 1 |
| | | NRC deep monitoring bore | 4.22 | 11.53 | 59.0 | 2 |
| | Wagener Golf Club | Deep monitoring bore | 3.42 | 4.48 | 69.0 | 4 |
| | Fishing Club at Houhora | Deep monitoring bore | 3.22 | 3.43 | 78.0 | 5 |
| Waiharara-Paparore Region | Kaimaumau Deep | NRC Monitoring Bore | 0.58 | 2.44 | 72.0 | 6 |
| | Ogle Drive | NRC Monitoring Bore | 1.45 | 14.90 | 68.0 | 3 |
| | Paparore | NRC deep monitoring bore | 4.03 | 6.88 | 75.0 | 6 |
| | | NRC deep monitoring bore | 4.08 | 6.88 | 65.0 | 4 |
| | | NRC middle monitoring bore | 4.88 | 6.46 | 35.0 | 2 |
| | | NRC shallow monitoring bore | 5.32 | 6.42 | 18.0 | 1 |
| | Valic-1 | Shallow Monitoring Bore | 1.85 | 21.74 | 17.0 | 1 |

| Model Region | Site | Piezometer Description | Root Mean Squared Error | Mean groundwater level (mAMSL) | Bore depth | Model Layer |
|---|---|---|---|---|---|---|
| | | Deep monitoring bore | 1.55 | 11.65 | 103.0 | 6 |
| | | Production Bore | 1.77 | 11.41 | 103.0 | 6 |
| | Valic-2 | Shallow Monitoring Bore | 1.80 | 22.88 | 55.0 | 1 |
| | | Deep monitoring bore | 1.21 | 12.24 | 121.0 | 6 |
| | | Production Bore | 1.19 | 12.06 | 121.0 | 6 |
| | Valic-3 | Shallow Monitoring Bore | 0.76 | 20.99 | 45.0 | 1 |
| | | Deep monitoring bore | 2.42 | 11.28 | 124.0 | 6 |
| | | Production Bore | 2.63 | 11.32 | 124.0 | 6 |
| | Valic-4 | Shallow Monitoring Bore | 0.76 | 20.99 | 45.0 | 1 |
| | | Deep monitoring bore | 2.42 | 11.28 | 124.0 | 6 |
| | | Production Bore | 1.77 | 10.75 | 93.0 | 6 |
| Sweetwater Farms Monitoring Wells | Sweetwater MW1 | Shallow Monitoring Bore | 2.77 | 13.84 | 13.3 | 1 |
| | | Deep monitoring bore | 4.98 | 2.83 | 94.0 | 6 |
| | Sweetwater MW2 | Shallow Monitoring Bore | 0.80 | 5.82 | 14.5 | 2 |
| | | Deep monitoring bore | 0.61 | 6.35 | 59.0 | 6 |
| | Sweetwater MW3 | Shallow Monitoring Bore | 0.34 | 7.61 | 5.0 | 1 |
| | | Deep monitoring bore | 1.82 | 5.83 | 47.0 | 6 |
| | Sweetwater MW4 | Shallow Monitoring Bore | 11.53 | 15.56 | 25.0 | 2 |
| | | Deep monitoring bore | 0.38 | 4.98 | 92.0 | 6 |
| | Sweetwater MW5 | Shallow Monitoring Bore | 4.99 | 15.09 | 6.0 | 1 |
| | | Deep monitoring bore | 0.95 | 8.67 | 61.0 | 6 |
| | Sweetwater MW6 | Shallow Monitoring Bore | 0.80 | 11.88 | 15.0 | 1 |
| | Sweetwater Nursery | Monitoring bore | 2.56 | 10.50 | 33.8 | 3 |
| Lake Heather Monitoring Bores | Lake Heather Piezometer 1 | NRC shallow monitoring bore | 0.82 | 11.97 | 26.0 | 1 |
| | | NRC deep monitoring bore | 0.70 | 8.04 | 105.5 | 6 |
| | Lake Heather Piezometer 2 | NRC shallow monitoring bore | 2.16 | 9.56 | 29.5 | 1 |
| | Lake Heather Piezometer 3 | NRC shallow monitoring bore | 1.24 | 13.11 | 29.0 | 1 |
| Private Bores in Southern Aupouri Aquifer | Vinac | Private bore | 2.34 | 0.04 | 33.0 | 4 |
| | Waipapa | Private bore | 1.61 | 2.93 | 56.0 | 4 |
| | Matich | Private bore | 1.46 | 4.73 | 0.0 | 1 |
| | Welch | Private bore | 0.90 | 8.12 | 31.7 | 3 |
| | Shanks | Private bore | 0.41 | 7.20 | Unknown | 1 |

The mean residual head is -0.08 m showing that there is not a strong bias for the simulations overpredicting or underpredicting observed groundwater levels. The mean of the RMSE for all gauges is 1.89 m, which is 7.1% of the observed range in groundwater head (26.5 m) while the RMSE for all observation in the model is 2.10 m, or 7.9 % of the range of observations. The latter number reflects a bias for gauges where more data is available whereas the former metric gives equal weight to a gauge with limited data. A simulated RMSE of less than 10% of the measured range is considered a good calibration so both analysis criteria meet this standard. Simulated and observed hydrographs for all monitoring wells used for model calibration are provided in **Appendix E**.

For the inland piezometers along the Hukatere transect in the Motutangi region (e.g. Hukatere and Forest), the trend of simulated groundwater level generally follows the observed groundwater level. However, the increase in groundwater levels over recent years has not been replicated in the simulation.

A potential reason for this is that variations in seasonal recharge rates have changed in response to land use. The groundwater model has been set up with recharge rates that were simulated based on a constant land use over the model period. However, land use changes and the associated spatial distributions of land cover will affect the quantity and quality of water being recharged to the groundwater system. In fact, the plantation forestry felling cycles on the western side of the peninsula may significantly affect the variation of groundwater recharge. In general, compared to bare land, forestry land tends to decrease the groundwater recharge due to increased interception and evapotranspiration.

Changes in land use take time to propagate to the groundwater system. Depending on the climate, geology, intensity and extent of the land use change, recovery of the groundwater system may vary from 3 to more than 20 years (Moore and Wondzell, 2005). In the meantime, this effect on groundwater system is masked by the climate variation.

It is therefore likely that the mismatch in calibration is in fact due to a temporal variation in groundwater recharge in response to land use change. However, detailed historical land cover data was not available. Reconstructing historical land use change would be a separate study in its own right and it was therefore not possible to incorporate the transient variability of recharge into the groundwater model to reflect the land use change in the area.

The Browne and Waterfront piezometers are generally well represented by the simulation, with good correlation of seasonal and annual trends, though in some cases, a discrepancy in water level elevation was observed. In some cases, this reflects the fact that piezometers at different depths correspond to the same model layer, for example the midpoint of the screened interval for Browne piezometers 2 and 3 are 16 and 29 m BGL, respectively, however both fall within model Layer 1 and therefore reflect the same simulation results.

Measured data at all deep aquifer bores at the Valic locations and at Ogle Drive were well represented by the model as evident in the hydrographs provided in **Appendix E**. Simulated groundwater levels at the deep bores in the Valic orchards are generally within 1 meter of measured values except Valic-3 where there is a greater discrepancy in earlier data; however, the last 5 years of the measured data set is similar to simulation results.

In the Waiharara-Paparore region the monitoring piezometer at Paparore is significantly oversimulated with measured groundwater levels typically 3 to 5 m above measured levels for each of the monitoring levels. The vertical hydraulic gradient was not well simulated indicating that a localised variation in permeability, reflecting the complex stratigraphy in the model area, may impede model calibration at this location as has been encountered in other modelling efforts (SKM, 2007b).

The monitoring bore at Ogle Drive was very well simulated in terms of temporal trends and the magnitude of seasonal water level variation. The overall simulated water level was 1 to 2 m below observed water levels.

Water levels were generally well simulated at the four Valic Orchards deep monitoring bores. At the shallow monitoring bore the simulated water levels were 2 to 3 m below observed levels, with the exception of Valic Monitoring Bore #3 where the simulated water level was similar to observations. A recent trend of declining groundwater levels in the Valic area was not well captured by the simulations, which may reflect land use changes not captured in the process of generating estimated recharge input into the model.

The discrepancy between simulated water levels in the shallow and deep monitoring bores around Valic Orchards shows that there are layers effecting the vertical hydraulic gradient that are not captured in the conceptual model.

A low permeability zone applied in Layer 2 of the model yielded some improvement in this regard, but it remains likely that the conceptual model does not capture some of the geologic complexity in this area.

In the southern portion of the model area the majority of monitoring wells are associated with Sweetwater Farms. There are 5 locations with paired shallow and deep monitoring piezometers and several additional single monitoring piezometers at Sweetwater Farms, as well as several bores where groundwater level data is collected by private land owners. Many of these data sets are limited in their historic extent.

In the case of the Sweetwater farms monitoring wells the vertical hydraulic gradient is not well captured in monitoring wells 1, 3, 4 and 5, though in the case of monitoring well 4 the shallow piezometer is likely measuring a perched water table based on the groundwater elevation being inconsistent with the general groundwater gradient in the surrounding area. The simulated water table is generally closer to observations in the case of the deep bores relative to the shallow monitoring wells due to the difficulty of representing the geologic complexity of the region within the constraints of the conceptual model.

### 4.4.2 Model Flow Budget

**Table 7** provides the long-term average water budget for the transient calibration model. The main input to the model is groundwater recharge at 80% of the total inflow. The predominant discharge component from the model are the subsurface coastal discharges, which are comprised of the constant head in Layer 1 (44%) and the GHB in Layer 2 to 6 (12%). Surface water discharges in the form of drains and wetlands account for 24% of the model water budget. Discharge through groundwater pumping is a small component (<1%) of the model water budget which reflects the fact that many of the large groundwater takes within the model were initiated in the last several years of the simulation period whereas the water balance presented in **Table 7** represents an average for the entire simulation period. At the time of peak irrigation over the simulation period, December 2010, groundwater pumping accounts for 4.9% of the groundwater budget.

Table 7. Average daily mass balance for 58-year simulation from 1/01/1960 to 31/07/2018.

| Mass balance | Components | Baseline Model | |
|---|---|---|---|
| | | Flow ($m^3/d$) | Percentage of Flow (%) |
| Inflow | Storage | 160,059 | 19.7 |
| | CH | 13 | 0.0 |
| | Recharge | 651,587 | 80.3 |
| | Lakes | 170 | 0.0 |
| | Cross Boundary Flow | NA | NA |
| | **Total inflow** | **811,828** | **100** |
| Outflow | Storage | 160,681 | 19.8 |
| | Shallow Coastal Discharge (CH) | 353,960 | 43.6 |
| | Wells | 5,668 | 0.7 |
| | Drains/Wetlands (DC) | 193,270 | 23.8 |
| | Deep Coastal Discharge (GHB) | 98,246 | 12.1 |
| | Cross Boundary Flow | NA | NA |
| | **Total outflow** | **811,825** | **100** |
| Percentage discrepancy | | 0.0% | |

Note: CH = constant head; GHB = general head boundary; DC = drain cells. Changes in storage are due to the difference in climatic and hence water table conditions between the start and the end of the model run.

# 5. Conclusions

A numerical groundwater flow model was developed for the Aupouri aquifer of Northland, New Zealand to be used to assess groundwater resources at the basin scale in the context of historic, present and future conditions. The calibrated model is intended to provide a tool for the evaluation of proposed groundwater extractions and its potential impact on both groundwater and surface water. In particular, the model can be used to define the potential impact from seasonal pumping on the aquifer system water budget, aquifer groundwater levels, surface water drain flows, and the position of the saltwater/fresh water interface.

**Model Development**

The framework for the model was based on review of all available borelogs, of which 198 were considered reliable enough to inform the development of the model stratigraphy. Geologic material noted in the borelogs was classified into four primary geologic layers; interbedded dune sand and peat, upper shellbed, compact sand, and lower shellbed; with the shellbed representing the aquifer material. The upper strata were sub-divided into 3 layers to account for the vertical heterogeneity in the material and allow for associated variability in conductivity and anisotropy to enable model calibration. The model layer base elevations were interpolated from the bore log data with the bottom of the lower shellbed being the lower model boundary.

Recharge to the model area was determined through an assessment of historic climate date and soil types processed using the SMWBM tool to develop a time series input based on historic rainfall and PET. Groundwater pumping was determined through an assessment of groundwater allocation over the model area and demand based on historic climate conditions.

**Model Calibration**

The model was calibrated to a historic dataset that included groundwater level observations measured at 56 locations. Each observation bore was assigned a model layer based on the depth of the bore and corresponding material within the model. A sensitivity analysis was performed to determine that hydraulic conductivity was the most sensitive model parameter, followed by vertical anisotropy.

The model was calibrated by systematically adjusting parameters in both a steady state and transient application to achieve the best possible agreement between simulated and measured water levels while maintaining realistic parameter values. In the case of the steady state simulation the parameter estimation tool, PEST, was used to determine the parameter values that best fit the observed data. These parameters were then used as the basis for the transient calibration.

The transient model was run for a simulation period of 58 years. A mean RMSE for all gauges of 1.89 m was achieved which was 7.1% of the range of observations. Many of the observation bores were well simulated in terms of their temporal trends while having a vertical displacement of the simulated water levels which may indicate the limitations of the 8 m DEM that was used to determine surface elevations in the model and subsequently the elevations of the model layers.

In some cases, vertical hydraulic gradients measured by nested piezometers were not well replicated in the simulation which reflects the limitations of capturing real world geologic complexity in a numerical model. Nonetheless model results indicate that the calibration is satisfactory for the intended application of the model.

**Water Budget**

Groundwater recharge in the Aupouri aquifer occurs through the percolation of rainfall and account for the majority of groundwater inflow. Groundwater outflows occur primarily as discharge to the coasts with some discharge also occurring as baseflow in streams and agricultural drains. Groundwater pumping is a small fraction of the overall groundwater budget; however, it has been increasing in recent years as groundwater allocation for agricultural use increases. At the time of peak irrigation total groundwater abstraction under current conditions accounts for 4.9% of the groundwater budget.

# 6. References

Edwards, M., 1996, Elimination of adaptive grid interface errors in the discrete cell centred pressure equation: Journal of Computational Physics, v. 126, article no. 0143, p. 356–372.

Isaac, M.J. (compiler), 1996: Geology of the Kaitaia area. Institute of Geological & Nuclear Sciences 1:250 000 geological map 1. 1 sheet + 43 p. Lower Hutt, New Zealand. GNS Science.

Lincoln Agritech, 2015. Aupouri Aquifer Review. Consultancy report prepared for Northland Regional Council.

Panday, Sorab, Langevin, C.D., Niswonger, R.G., Ibaraki, Motomu, and Hughes, J.D., 2013, MODFLOW–USG version 1: An unstructured grid version of MODFLOW for simulating groundwater flow and tightly coupled processes using a control volume finite-difference formulation: U.S. Geological Survey Techniques and Methods, book 6, chap. A45, 66 p

SKM, 2007a. Awanui Artesian Aquifer Numerical Modelling. Consultancy report prepared for Northland Regional Council.

SKM, 2007b. King Avocado Orchard Groundwater Take Consent Application (AEE Final). Consultancy report prepared for King Avocado Limited.

SKM, 2010. Sweetwater Station Water Take Hearing - Response to Section 92 request. Consultancy report prepared for Landcorp Farming Limited and Te Runanga O Te Rarawa.

Van Genuchten, M. Th. 1980. A closed-form equation for predicting the hydraulic conductivity of unsaturated soils. Soil. Sci. Soc. Am. J. 44:892—898.

Moore, R., & Wondzell, S. M. (2005). Physical hydrology and the effects of forest harvesting in the Pacific Northwest: a review. JAWRA Journal of the American Water Resources Association, 41(4), 763-784.Mulder, P. J. M. 1983. Rapportage putproef Hoogezand. Dienst Grondwaterverkenning TNO, Delft, OS.83 – 24, 7p.

Mulder, P.J.M. 1983. Rapportage putproef Hoogezand. Dienst Grondwaterverkenning TNO Delft

Williamson Water Advisory (2017). Motutangi-Waiharara Groundwater Model Factual Technical Report. Consultancy report prepared for Motutangi-Waiharara Water User Group.

Williamson Water Advisory (2018). Waiharara-Paparore Groundwater Model Factual Technical Report. Consultancy report prepared for Valic Avocados ltd, Tiri Orchards ltd, Wataview Orchard

Williamson Water Advisory (2018). Sweetwater Farms PB2 Test Pumping Report. Consultancy Report prepared for Sweetwater Farms Limited.

# Appendix A. Summary of Aquifer Hydraulic Properties

The following tables summarise hydraulic property values that have been measured and estimated in models across the Aupouri Peninsula from various reports since 2000.

Table A1. Analysis of aquifer test data (Lincoln Agritech, 2015).

| Pump | Screen depth | Test name | Lithology | T | B | Kx | S | K'/B' | B' | K'z |
|---|---|---|---|---|---|---|---|---|---|---|
| | (mBGL) | | | ($m^2$/d) | (m) | (m/d) | (-) | (d) | (m) | (m/d) |
| 200048 | 18.8 | Hukatere 1 | Sand | 60 | 6.4 | 9.4 | 0.0017 | 0.1475 | 13.5 | 2.0 |
| 200048 | 18.8 | Hukatere 1 | Sand | 60 | 6.4 | 9.4 | 0.0107 | 0.2927 | 13.5 | 4.0 |
| 200048 | 18.8 | Hukatere 3 | Sand | 50 | 6.4 | 7.8 | 0.0022 | 0.1909 | 13.5 | 2.6 |
| 200048 | 18.8 | Hukatere 3 | Sand | 62 | 6.4 | 9.7 | 0.0154 | 0.1909 | 13.5 | 2.6 |
| 200060 | 64 | Browne | Sand | 400 | 10.4 | 38.5 | 0.0004 | 0.0014 | 21.2 | 0.03 |
| 200081 | 31.2 | Ogle Drive | Sand | 7.4 | 8.1 | 0.9 | 0.0467 | 0.8771 | 10.2 | 8.9 |
| 200229 | 73 | Fitzwater | Shell/sand | 130 | 6 | 21.7 | 0.0002 | 0.0001 | 26.0 | 0.004 |
| 200229 | 73 | Fitzwater | Shell/sand | 110 | 6 | 18.3 | 0.0004 | 0.0004 | 11.0 | 0.004 |
| 201025 | 27 | Sweetwater | Sand | 52 | 6.3 | 8.3 | 0.0004 | 0.0018 | 11.0 | 0.02 |
| 201037 | 27.2 | Welch | Sand/shell | 9 | 1.8 | 5 | 0.0005 | 0.0087 | 11.9 | 0.1 |
| 209606 | 110.5 | King Avo | Shell | 305 | 26 | 11.7 | 0.0007 | 0.0003 | 15.5 | 0.004 |
| 209606 | 110.5 | King Avo | Shell | 370 | 17 | 21.8 | 0.0011 | 0.0003 | 15.8 | 0.005 |
| | | | **Min** | 7.4 | 1.8 | 0.9 | 0.0002 | 0.0001 | 10 | 0.004 |
| | | | **Mean** | 135 | 8.9 | 13.5 | 0.0067 | 0.14 | 15 | 1.7 |
| | | | **Max** | 400 | 26 | 38.5 | 0.0467 | 0.88 | 26 | 8.9 |

Table A2. Analysis of aquifer test data (HydroGeo Solutions, 2000).

| NRC Bore | Depth | Top of screen | Aquifer type | SWL | T | K | S |
|---|---|---|---|---|---|---|---|
| | (m) | (mBGL) | | (mBGL) | ($m^2$/d) | (m/s) | (-) |
| 43 | 55 | 52 | Fine sand | 9.3 | 240 - 280 | 6E-05 to 7.1E-05 | - |
| 48 | 67 | 19 | Med sand | 5.3 | 80 - 300 | 6.1E-05 to 7.1E-05 | 0.01-0.001 |
| 59 (s) | 6 | - | Fine sand | 2.8 | 140 | 5.10E-04 | - |
| 59 (d) | 55 | 49 | Fine sand | 13.4 | 190 | 5.30E-05 | - |
| 60 | 60 | - | Fine sand | 14.9 | 220 - 850 | 5.6E-06 to 1.3E-04 | - |
| 81 | 32 | 31 | Fine sand | 20.9 | 12 - 28 | 1.25E-05 to 2.9E-05 | 0.07-0.03 |
| 152 | 66 | 60 | Fine sand | 30.1 | 260 | 8.40E-05 | - |
| 184 | 110 | 101 | Shelly sand | 17.2 | 140 -340 | 1.7E-05 to 4.2E-05 | - |
| 229 (211) | 79 | 70 | Shelly sand | 2.6 | 140 | 2.10E-05 | 1.4E-04 to 1.8E-03 |
| 230 | 88 | 63 | Shelly sand | 4.6 | 240 - 310 | 4.3E-05 to 3.3E-05 | - |

| NRC Bore | Depth | Top of screen | Aquifer type | SWL | T | K | S |
|---|---|---|---|---|---|---|---|
| | (m) | (mBGL) | | (mBGL) | ($m^2$/d) | (m/s) | (-) |
| 1007 | 50 | 45 | Fine sand | 33.7 | 275 -305 | 2.1E-04 to 1.9E-04 | - |
| 1025 | 30 | 27 | Fine sand | 1.55 | 60 -103 | 2.2E-05 to 3.7E-05 | 2.5E-04 to 5.0E-04 |
| 1374 | 32 | 26.6 | Fine sand | 0.8 | 48 | 1.80E-05 | 1.0E-05 to 2.0E-05 |
| 1424* | 82 | 70 | - | - | 260 | - | - |

Table A3. Summary of aquifer test data (SKM, 2010).

| Bore Owner | Well ARC No | Easting (NZMG) | Northing (NZMG) | Test Type | Test Dur. (hrs) | Rate ($m^3$/day) | Obs. Bores | Screen Geology | K (m/s) | Information Source |
|---|---|---|---|---|---|---|---|---|---|---|
| King | 201374 | 2533400 | 6681500 | Constant Rate | 24 | 576 | Yes (1) | Shell | 1.8E-05 | HydroGeo Solutions (2000) |
| Sweetwater Orchards | 201424 | 2529558 | 6684434 | Constant Rate | 72 | 1,176 | Yes (1) | Shell | 1.9E-04 | Woodward Clyde (1998) |
| Kaurex Corporation | 200230 | 2530331 | 6697328 | Constant Rate | 9.5 | 273 | No (PB only) | Shell | 4.3 – 3.3E-05 | HydroGeo Solutions (2000) |
| Matai Orchards | 201507 | 2529399 | 6691299 | Constant Rate | 88.5 | 497 | Yes (1) | Shell | 4.0 – 2.0E-04 | SKM (2007) |
| Hopkins | 200184 | 2520300 | 6706800 | Constant Rate | 24 | 260 | No (PB only) | Shell | 4.2 – 1.7E-05 | HydroGeo Solutions (2000) |
| Fitzwater | 200229 | 2529743 | 6690648 | Constant Rate | 24 | 864 | Yes (4) | Shell | 2.1 – 1.4E-04 | HydroGeo Solutions (2000) and SKM (2007) |
| Brown | 200060 | 2521699 | 6706300 | Constant Rate | 22 | 708 | Yes (3) | Sand | 5.6E-06 – 1.3E-04 | HydroGeo Solutions (2000) |
| Hogg | 201007 | 2528300 | 6685799 | Constant Rate | 20.9 | 160 | No (PB only) | Sand | 2.1 – 1.9E-04 | HydroGeo Solutions (2000) |
| Waiharara | 209499 | 2528580 | 6690100 | Constant Rate | 91 | 1,113 | Yes (2) | Shell | 2.0E-04 | SKM (2007) |
| King Avocado Ltd | 209606 | 2527482 | 6690562 | Constant Rate | 168 | 2,393 | Yes (3) | Shell | 4.3 – 1.5E-04 | SKM (2007) |
| Hamilton Nurseries | 201025 | 2531401 | 6684155 | Constant Rate | 6 | 300 | Yes (2) | Sand | 1.2E-04 | SKM (2001) |
| Stanisich Orchard | 200192 | 2528600 | 6695799 | Constant Rate | 1 | 1,442 | No (PB only) | Shell | 5.0E-05 | SKM (2002a) |
| Terra Nova Orchard | 200335 | 2521199 | 6706499 | Constant Rat | 39 | 674 | Yes (6) | Shell | 4.0 – 3.0E-04 | SKM (2002b) |
| Northland Catchment Commission | 200048 | 2519855 | 6701857 | N/A | N/A | N/A | N/A | Sand | 7.1 – 6.1E-05 | HydroGeo Solutions (2000) |
| Northland Catchment Commission | 200081 | 2528583 | 6689795 | N/A | N/A | N/A | N/A | Sand | 2.9 – 1.25E-05 | HydroGeo Solutions (2000) |

| | | | | | | | | | | |
|---|---|---|---|---|---|---|---|---|---|---|
| Colville | 200059 | 2521792 | 6705887 | Step (4) | 22.3 | 63 - 233 | No (PB only) | Sand | 5.3E-05 | HydroGeo Solutions (2000) |
| Fraser | 201002 | 2525552 | 6671053 | Step (3) | 22 | 89 - 163 | No (PB only) | Sand | 3.0E-04 | NRC database |
| Richards Enterprises | 200043 | 2522513 | 6708792 | Step (4) | 19 | 149 -333 | No (PB only) | Sand | 7.1 – 6.0E-05 | HydroGeo Solutions (2000) |
| Herbert | 200152 | 2528178 | 6688977 | Step (4) | 20 | 127 - 319 | No (PB only) | Sand | 8.4E-05 | HydroGeo Solutions (2000) |

Table A4. Calibrated model parameters (SKM, 2007a).

| Material ID | Hydraulic Conductivity | | Vertical anisotropy | Sy |
|---|---|---|---|---|
| | (m/d) | (m/s) | (-) | (-) |
| Loose dune sand | 10 | 1.20E-04 | 10 | 0.2 |
| Weathered dune sand | 6 | 6.90E-05 | 10 | 0.2 |
| Fine sand | 3 | 3.50E-05 | 25 | 0.25 |
| Peat and sand | 0.1 | 1.20E-06 | 30 | 0.2 |
| Upper alluvium | 0.55 | 6.40E-06 | 10 | 0.3 |
| Alluvium | 0.06 | 6.90E-07 | 20 | 0.05 |
| Shellbed | 50 | 5.80E-04 | 2 | 0.3 |

Table A5. Aquifer hydraulic parameters derived from SKM102PB test pumping (SKM, 2007b).

| Bore | T | K | |
|---|---|---|---|
| | ($m^2$/s) | (m/d) | (m/s) |
| SKM101b | 3.70E-03 | 32 | 3.70E-04 |
| SKM102b | 1.50E-03 | 13 | 1.50E-04 |
| SKM103b | 3.50E-03 | 30 | 3.50E-04 |
| SKM104b | 4.30E-03 | 37 | 4.30E-04 |

Table A6. Material parameters used within PLAXIS geotechnical subsidence model (SKM, 2007b).

| King Avocado Orchard Groundwater Take Consent Application (AEE Final) | | | | | | | |
|---|---|---|---|---|---|---|---|
| Material | Density (KN/$m^{3)}$ | | Permeability (m/d) | | Stiffness (kN/$m^2$) | Cohesion (kN/$m^2$) | Friction Angle (°) |
| | δunsat | δsat | Kx | Ky | E50ref | cref | ø |
| Loose Dune Sand | 15 | 17 | 5 | 0.25 | 10000 | 0.2 | 28 |

| | | | | | | | |
|---|---|---|---|---|---|---|---|
| Compact Dune Sand | 17 | 19 | 0.7 | 0.07 | 15000 | 0.2 | 28 |
| Shellbed | 18 | 20 | 22 | 2.2 | 30000 | 1 | 30 |

Table A7. Hydrogeological data calculated from pumping tests (WWA, 2017).

| Farm | Rate (L/s) | Bore | Screen Depth (mBGL) | Method | T ($m^2/d$) | S (-) | B (m) | K (m/d) | K (m/s) |
|---|---|---|---|---|---|---|---|---|---|
| Stanisich Farm | 25 | Pumping bore | 87-101 | Single well Jacob | 485 | - | 14 | 35 | 4.1E-04 |
| | | | | Theis Recovery | 512 | - | | 37 | 4.3E-04 |
| | - | Monitoring bore | 77-85 | Theis (point match) | 356 | 0.0044 | 8 | 45 | 5.2E-04 |
| Honeytree Farm | 29 | Pumping bore | 62-68, 68-71,84-93 | Single well Jacob | 618 | - | 18 | 34 | 3.9E-04 |
| | | | | Theis Recovery | 511 | - | | 28 | 3.2E-04 |
| | - | Monitoring bore | 63-69, 69-72,86-95 | Theis (point match) | 751 | 0.0003 | 18 | 42 | 4.9E-04 |
| | | | | Cooper Jacob | 784 | 0.0003 | | 44 | 5.1E-04 |
| De Bede Farm | 2.3 | Pumping bore | 91-97 | Single well Jacob | 377 | - | 6 | 63 | 7.3E-04 |
| | | | | Theis Recovery | 363 | - | | 61 | 7.1E-04 |
| | | | | **Max** | 784 | 0.0044 | | 63 | 7.3E-04 |
| | | | | **Min** | 356 | 0.0003 | | 28 | 3.2E-04 |
| | | | | **Mean** | 528 | 0.0016 | | 43 | 5.0E-04 |

Table A8. Calculated hydrogeological property from Single well Jacob method (WWA, 2017).

| Farm | Q (L/s) | Bore | Screen Depth (mBGL) | Evaluation time (s) | T ($m^2/d$) | B (m) | K (m/d) | K (m/s) | Time (s) evaluation criteria | |
|---|---|---|---|---|---|---|---|---|---|---|
| | | | | | | | | | Minimum | Maximum |
| Stanisich | 25 | Pumping bore | 87-101 | 210 - 1200 | 471 | 14 | 34 | 3.9E-04 | 183 | 1728 |
| De Bede | 2.3 | Pumping bore | 91-97 | 330 - 1470 | 273 | 6 | 46 | 5.3E-04 | 86 | 1728 |

Table A9. Estimated hydrogeological parameters from Hantush – Jacob method (WWA, 2017).

| Bore | T | $K_h$ | $K_h$ | K'/B' | $S_s$ |
|---|---|---|---|---|---|
| | $m^2/d$ | m/d | m/s | $d^{-1}$ | $m^{-1}$ |
| Stanisich observation bore 2 (monitoring bore) | 138 | 10 | 1.14E-04 | 1.83E-03 | 1.55E-04 |
| | 408 | 29 | 3.38E-04 | 1.35E-03 | 3.07E-04 |
| | 348 | 25 | 2.88E-04 | 7.36E-04 | 3.13E-04 |
| Honeytree farm production bore 1(monitoring bore) | 579 | 32 | 3.72E-04 | 1.50E-04 | 1.63E-05 |
| | 484 | 27 | 3.11E-04 | 2.84E-04 | 2.17E-05 |
| | 707 | 39 | 4.54E-04 | 5.09E-05 | 1.70E-05 |

Table A10. Calibrated Model Parameters (WWA, 2017).

| Model Geological Units | Model Layer | $K_x$ | | Vertical Anisotropy | $S_y$ | $S_s$ |
|---|---|---|---|---|---|---|
| | | (m/d) | (m/s) | (-) | (-) | ($m^{-1}$) |
| Coastal sand | 1 | 4.5 | 5.2E-05 | 70 | 0.3 | - |
| Weathered sand | 1 | 2.8 | 3.2E-05 | 90 | 0.25 | - |
| Plain zone | 1 | 0.1 | 1.2E-06 | 15 | 0.01 | - |
| Coastal sand | 2&3 | 4 | 4.6E-05 | 30 | - | 0.0005 |
| Weathered sand | 2&3 | 3 | 3.5E-05 | 80 | - | 0.0005 |
| Shellbed | 4 | 35 | 4.1E-04 | 1 | - | 0.0016 |
| Sand | 5 | 6 | 6.9E-05 | 30 | - | 0.0005 |
| Shellbed | 6 | 22 | 2.5E-04 | 1 | - | 0.0016 |

Table A11. Test pumping results for Sweetwater Farms (WWA, 2018).

| Test | Analysis | Pumping rate | | Screen length | Transmissivity (T) | Hydraulic conductivity (K) | Specific storage (/m) |
|---|---|---|---|---|---|---|---|
| | | L/s | $m^3/d$ | m | $m^2/d$ | m/s | |
| Constant pumping | PB6 Cooper-Jacob | 64 | 5,495 | 17 | 5,700 | 3.9E-03 | 9.6E-04 |
| | PB2 Cooper-Jacob | 64 | 5,495 | 17 | 430 | 2.9E-04 | - |
| Recovery | PB2 Theis | 64 | 5495 | 17 | 354 | 2.4E-04 | - |

# Appendix B. Recharge Modelling

## B.1 Model Parameters

The soil moisture water balance model (SMWBM) is a deterministic lumped parameter model originally developed by Pitman (1976) to simulate river flows in South Africa. The code was reworked into a Windows environment and the functionality extended to include a surface ponding function, additional evaporation functions and an irrigation module.

The model utilises daily rainfall and potential evaporation data to calculate soil moisture conditions and the various components of the catchment water balance under natural rainfall or irrigated conditions. The model operates on a time-step with a maximum length of daily during dry days, with smaller hourly time-steps implemented on wet days.

The model incorporates parameters that characterise the catchment in terms of:

- interception storage,
- evaporation losses,
- soil moisture storage capacity,
- plant available water capacity,
- soil infiltration,
- sub-soil drainage;
- vadose zone vertical drainage'
- surface runoff (quickflow);
- stream baseflows (groundwater contribution); and
- the recession and/or attenuation of groundwater and surface water flow components, respectively.

## B.2 Fundamental Operation

The fundamental operation of the model is as follows and in **Table B1**:

When a rainday occurs, daily rainfall is disaggregated into the hourly time-steps based on a pre-defined synthetic rainfall distribution, which includes peak intensities during the middle of the storm. This time stepping approach ensures that rainfall intensity effects and antecedent catchment conditions are considered in a realistic manner by refined accounting of soil infiltration, ponding and evaporation losses.

Rainfall received must first fill a nominal interception storage (PI – see below) before reaching the soil zone, where the net rainfall is assessed as part of the runoff/infiltration calculation.

Water that penetrates the soil fills a nominal soil moisture storage zone (ST). This zone is subject to evapotranspiration via root uptake and direct evaporation (R) according to the daily evaporation rate and current soil moisture deficits. The soil moisture zone provides a source of water for deeper percolation to the underlying aquifer, which is governed by the parameters FT and POW.

If disaggregated hourly rainfall is of greater intensity than the calculated hourly infiltration rate (ZMAX, ZMIN) surface runoff occurs. Surface runoff is also governed by two other factors, which are the prevailing soil moisture deficit and the proportion of impervious portions of the catchment directly linked to drainage pathways (AI).

Rainfall of sufficient intensity and duration to fill the soil moisture storage results in excess rainfall that is allocated to either surface runoff or groundwater percolation depending on the drainage and slope characteristics of the catchment (DIV).

Finally, the model produces daily summaries of the various components of the catchment water balance and calculates the combined surface runoff/percolation to groundwater to form a total catchment discharge.

Table B1. Summary of SMWBM parameters and value assignments for this study.

| Parameter | Name | Parameter Values | | | Description |
|---|---|---|---|---|---|
| | | Coastal sand | Weather-ed sand | Plain zone | |
| ST (mm) | Maximum soil water content. | 178.5 | 178.5 | 100 | ST defines the size of the soil moisture store in terms of a depth of water. ST is approximately equivalent to root zone depth divided by soil porosity. |
| SL (mm) | Soil moisture content where drainage ceases. | 0 | 0 | 0 | Soil moisture storage capacity below which sub-soil drainage ceases due to soil moisture retention. |
| ZMAX (mm/hr) | Maximum infiltration rate. | 20 | 20 | 5 | ZMAX and ZMIN are nominal maximum and minimum infiltration rates in mm/hr used by the model to calculate the actual infiltration rate ZACT. ZMAX and ZMIN regulate the volume of water entering soil moisture storage and the resulting surface runoff. ZMIN is usually assigned zero. ZMAX is usually assigned the saturated infiltration rate from field testing. ZACT may be greater than ZMAX at the start of a rainfall event. ZACT is usually nearest to ZMAX when soil moisture is nearing maximum capacity. |
| ZMIN (mm/hr) | Minimum infiltration rate. | 0 | 0 | 0 | |
| FT (mm/day) | Sub-soil drainage rate from soil moisture storage at full capacity. | 5 | 3.8 | 0.8 | Together with POW, FT (mm/day) controls the rate of percolation to the underlying aquifer system from the soil moisture storage zone. FT is the maximum rate of percolation through the soil zone. |
| POW (>0) | Power of the soil moisture-percolation equation. | 2 | 2 | 2 | POW determines the rate at which sub-soil drainage diminishes as the soil moisture content is decreased. POW therefore has significant effect on the seasonal distribution and reliability of drainage and hence baseflow, as well as the total yield from a catchment. |
| AI (-) | Impervious portion of catchment. | 0 | 0 | 0.01 | AI represents the proportion of impervious zones of the catchment directly linked to drainage pathways. |
| R (0,1,10) | Evaporation-soil moisture relationship | 0 | 0 | 0 | Together with the soil moisture storage parameters ST and SL, R governs the evaporative process within the model. Three different relationships are available. The rate of evapotranspiration is estimated using either a linear (0,1) or power-curve (10) relationship relating evaporation to the soil moisture status of the soil. As the soil moisture capacity approaches full, evaporation occurs at a near maximum rate based on the mean monthly pan evaporation rate, and as the soil moisture capacity decreases, evaporation decreases according to the predefined function. |
| DIV (-) | Fraction of excess rainfall allocated directly to pond storage. | 0 | 0 | 0 | DIV has values between 0 and 1 and defines the proportion of excess rainfall ponded at the surface due to saturation of the soil zone or rainfall exceeding the soils infiltration capacity to eventually infiltrate the soil, with the remainder (and typically majority) as direct runoff. |
| Kv (m/s) | Vertical hydraulic conductivity | 8E-6 | 5E-6 | 2E-8 | Kv along with the VGn parameter and the soil moisture status governs the unsaturated hydraulic conductivity and travel times within the vadose zone. |

| Parameter | Name | Parameter Values | | | Description |
|---|---|---|---|---|---|
| | | Coastal sand | Weather-ed sand | Plain zone | |
| VGn (-) | van Genuchten parameter | 2.68 | 2.68 | 1.09 | Defines the soil moisture to unsaturated conductivity relationship according to van Genuchten's equation. |
| VPor (-) | Average porosity of the vadose zone | 0.15 | 0.15 | 0.40 | This is typically fixed and not changed during calibration as changes can easily be compensated for in Kv. |
| D (m) | Average depth of the vadose zone | 10 | 10 | 1 | The deeper the vadose zone, the longer the travel times. |
| TL (days) | Routing coefficient for surface runoff. | 1 | 1 | 1 | TL defines the lag of surface water runoff. This is not necessary to define for this study as we are only interested in the groundwater percolation component of the water balance. |
| GL | Groundwater recession parameter. | 1 | 1 | 1 | GL governs the lag in groundwater discharge or baseflow from a catchment. |

## B.3 Vadose zone discharge functionality

Based on the simulated groundwater percolation from the soil moisture model, the vadose zone discharge functionality was utilised to simulate the vertical movement of water in the unsaturated zone. The depth and hydraulic properties of the vadose zone govern the delay in groundwater response to climate variation.

The vadose zone functionality built into the SMWBM is premised on three principals:

1. ***Unsaturated hydraulic conductivity -*** The van Genuchten (1980) equation was used to determine unsaturated hydraulic conductivity in the vadose zone, which is governed by the saturated hydraulic conductivity that sets the upper value, and the degree of saturation in the soil zone as a proxy for general sub-surface degree of wetness.

2. ***Vertical flux rate*** - The simplified Richard's equation is used to estimate the vertical flux rate of water, which is assumed to be driven by gravitational force (only) and therefore governed by unsaturated hydraulic conductivity and porosity.

3. ***Transport time*** - The Muskingum equation was used to translate the vertical flux into a routing scheme, using the depth of the vadose zone and vertical flux rate (velocity) as the time component of the equation.

The delay in groundwater recharge was observed for coast sand, weathered sand and peat and clay to different extents. The simulated results for weathered sand suggest that the groundwater recharge has approximately 2-3 months delay in responding to the rainfall variation, depending on locality. **Figure B1.** provides an example of the functionality of the vadose zone model.

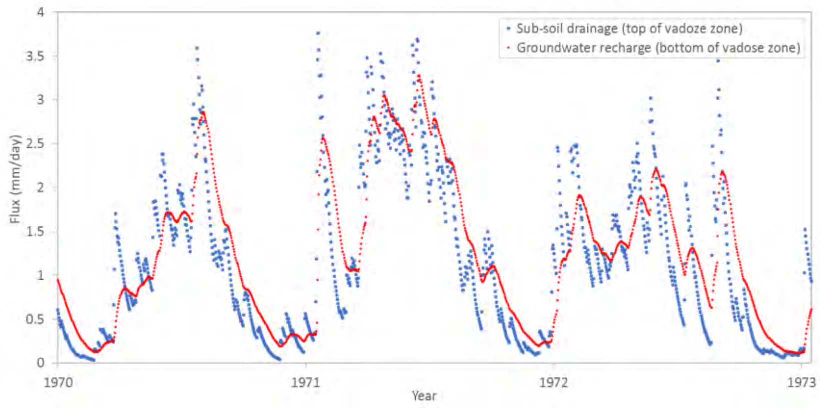


Figure B1. Graph comparing inputs and outputs from vadose zone model.

# Appendix C. Groundwater Takes

All groundwater takes incorporated in the model are listed in **Table C1** through **Table C3**. Bores with figure reference identification numbers beginning with "C" are for bores with a consented groundwater take. Bores with figure reference identification numbers beginning with "P" are for bores with a proposed groundwater take.

Table C1. Consented and proposed groundwater users in Northern portion of the model corresponding to Figure 9A

| Figure reference | IRISID (where available) | Bore Owners | Groundwater Take-Consented Total ($m^3$/yr) | Groundwater Take per Bore ($m^3$/yr) | X coordinate | Y coordinate |
|---|---|---|---|---|---|---|
| C1 | | Henderson Bay Avocados-Consented | 13,000 | 13,000 | 1605547 | 6154694 |
| C2 | | Waikopu Avocados-Consented | 44,640 | 44,640 | 1604046 | 6153129 |
| C3 | AUT.029091.01.01 | G J & D J Price | 7,500 | 7,500 | 1606898 | 6152070 |
| C4 | AUT.003768.01.04 | L & P Trust | 6,000 | 6,000 | 1606061 | 6149936 |
| C5 | APP.039244.01.01 | Kelvin Thomas* | 59,600 | 59,600 | 1610222 | 6147542 |
| C6 | AUT.037292.01.01 | Fullam GW take | 14,000 | 14,000 | 1609975 | 6147378 |
| C7 | APP.039381.01.01 | Brien Lamb* | 14,900 | 14,900 | 1610058 | 6147313 |
| C8 | AUT.002890.01.02 | LL & DF Rasmussen | 43,200 | 43,200 | 1611481 | 6146609 |
| C8 | AUT.004543.01.03 | Wagener Houhora Heads Properties Ltd | 45,000 | 45,000 | 1612372 | 6145137 |
| C9 | AUT.003883.01.03 | Longbeach Trust | 26,400 | 26,400 | 1610973 | 6145083 |
| C10 | AUT.003841.01.02 | Tomo Orchard Ltd | 14,800 | 14,800 | 1610945 | 6144743 |
| C11 | AUT.008203.01.02 | Ongare Trust-2 | 55,056 | 37,200 | 1611610 | 6144688 |
| C12 | AUT.026611.01.01 | Alligator Pear Partnership | 49,752 | 49,752 | 1611191 | 6144687 |
| C13 | APP.039345.01.01 | McLarnon-Ongare trust* | 23,520 | 23,520 | 1611284 | 6144679 |
| C14 | AUT.012472.01.01 | Ongare Trust-1 | 55,056 | 17,856 | 1611345 | 6144535 |
| C15 | AUT.009808.01.02 | B C Smith | 51,200 | 51,200 | 1610575 | 6144488 |
| C16 | AUT.020726.02.02 | E J Williams | 33,000 | 33,000 | 1610309 | 6144289 |
| C17 | AUT.028511.01.02 | Far North Avos Limited | 32,000 | 32,000 | 1610547 | 6144269 |
| C18 | | Far North Avocados (Blake Powell) - Consented | 32,000 | 32,000 | 1610547 | 6144269 |
| C19 | AUT.020727.02.02 | Honeytree Farms Ltd | 33,000 | 33,000 | 1610360 | 6144161 |
| C20 | AUT.023557.01.02 | Whispering Pines Ltd | 46,000 | 46,000 | 1611525 | 6144087 |
| C21 | AUT.003726.01.02 | Hine & Associates current | 74,400 | 74,400 | 1610798 | 6144048 |
| C22 | AUT.008605.01.02 | Trebcombe Limited-1 | 78,120 | 52,080 | 1611216 | 6143980 |
| C23 | AUT.007735.01.04 | S127 GW take | 66,000 | 66,000 | 1610514 | 6143937 |
| C24 | AUT.038075.01.01 | McQuarrie | 12,000 | 12,000 | 1611559 | 6143858 |
| C25 | AUT.003527.01.02 | Trebcombe Limited-2 | 78,120 | 26,040 | 1610842 | 6143760 |
| C26 | AUT.003888.01.02 | RB Freeman-1 | 60,480 | 34,560 | 1611320 | 6143725 |
| C27 | AUT.008586.02.01 | EJ Wagener | 30,000 | 30,000 | 1611836 | 6143656 |
| C28 | AUT.007108.01.02 | Matalaka Trust | 16,740 | 16,740 | 1610610 | 6143652 |

| Figure reference | IRISID (where available) | Bore Owners | Groundwater Take-Consented Total ($m^3/yr$) | Groundwater Take per Bore ($m^3/yr$) | X coordinate | Y coordinate |
|---|---|---|---|---|---|---|
| C29 | AUT.003372.01.02 | RB Freeman-2 | 60,480 | 25,920 | 1610829 | 6143550 |
| C30 | AUT.037274.01.01 | Whalers Rd Houhora | 74,500 | 74,500 | 1611997 | 6143025 |
| C31 | AUT.036910.01.02 | Soltysik-Freeman Fam Trust | 135,000 | 135,000 | 1611801 | 6142975 |
| C32 | APP.038732.01.01 | Valadares* | 22,350 | 22,350 | 1611872 | 6142927 |
| C33 | partial | Mapua Avocados-1 | 418,000 | 139,333 | 1612784 | 6142645 |
| C34 | partial | Mapua Avocados-2 | 418,000 | 139,333 | 1612979 | 6142360 |
| P1 | | Henderson Bay Avocados | 19,000 | 19,000 | 1605623 | 6154872 |
| P2 | | Far North Avocados (Blake Powell) | 32,000 | 32,000 | 1605981 | 6154581 |
| P3 | | Waikopu Avocados | 83,360 | 83,360 | 1603347 | 6153388 |
| P4 | | Te Raite Station_Waihopo | 120,000 | 60,000 | 1605333 | 6151462 |
| P5 | | Te Raite Station_other | 157,500 | 157,500 | 1603898 | 6151179 |
| P6 | | Te Raite Station_Waihopo | 120,000 | 78,750 | 1607102 | 6150752 |
| P7 | | Te Raite Station-Hourhora | 875,000 | 125,000 | 1608383 | 6148854 |
| P8 | | J. Evans | 160,000 | 160,000 | 1609502 | 6148854 |
| P9 | | Te Raite Station-Hourhora | 875,000 | 125,000 | 1609287 | 6148271 |
| P10 | APP.040652.01.01 | S. & L. Blucher | 96,000 | 96,000 | 1610145 | 6148091 |
| P11 | | Te Raite Station-Hourhora | 875,000 | 125,000 | 1607182 | 6148084 |
| P12 | | Te Raite Station-Hourhora | 875,000 | 125,000 | 1607771 | 6147949 |
| P13 | | Te Raite Station-Hourhora | 875,000 | 125,000 | 1609016 | 6147852 |
| P14 | | Te Raite Station-Hourhora | 875,000 | 125,000 | 1609296 | 6147373 |
| P15 | | Te Raite Station-Hourhora | 875,000 | 125,000 | 1609655 | 6147078 |
| P16 | APP.040397.01.01 | A. Matthews | 12,000 | 12,000 | 1611037 | 6146088 |
| P17 | APP.039644.01.01 | D. Wedding & Doody | 304,000 | 304,000 | 1610296 | 6145329 |
| P18 | APP.040121.01.01 | M. Evans | 36,400 | 36,400 | 1610444 | 6144926 |
| P19 | | Temp Consent for M Evans (only 1 year) | 24,000 | 9,100 | 1610444 | 6144926 |

*Members of the Motutangi Water Users Group. Applications have been consented but are unexercised as of the completion of this report.

Table C2. Consented and proposed groundwater users in Northern portion of the model corresponding to Figure 9B

| Figure reference | IRISID (where available) | Bore Owners | Groundwater Take-Consented Total ($m^3$/yr) | Groundwater Take per Bore ($m^3$/yr) | X coordinate | Y coordinate |
|---|---|---|---|---|---|---|
| C36 | AUT.008340.01.03 | Shirttail Orchards | 158,520 | 158,520 | 1613554 | 6140038 |
| C37 | AUT.003964.01.03 | Subritzky | 67,106 | 67,106 | 1614010 | 6139855 |
| C38 | AUT.038379.01.01 | De Bede | 70,000 | 70,000 | 1615069 | 6139351 |
| C39 | APP.039332.01.01 | Candy Corn Ltd* | 78,400 | 78,400 | 1614723 | 6139203 |
| C40 | APP.038589.01.01 | Thompson* | 35,280 | 35,280 | 1614798 | 6138773 |
| C41 | AUT.008647.01.03 | KSL Ltd | 52,800 | 52,800 | 1614554 | 6138575 |
| C42 | APP.038591.01.01 | Cypress Hills Ltd1* | 35,280 | 35,280 | 1614898 | 6138495 |
| C43 | AUT.028834.01.01 | JR Avocados Ltd | 20,000 | 20,000 | 1614800 | 6138422 |
| C44 | partial | GT&MT Covich-1 | 223,500 | 111,750 | 1617353 | 6136859 |
| C45 | APP.038410.01.01 | GT&MT Covich-2* | 223,500 | 111,750 | 1617128 | 6136793 |
| C46 | partial | Honeytree2 | 346,425 | 173,213 | 1618611 | 6136321 |
| C47 | APP.038471.01.01 | Honeytree1* | 346,425 | 173,213 | 1618903 | 6136060 |
| C48 | APP.038513.01.01 | Ngai Takakto1* | 193,700 | 96,850 | 1618987 | 6135795 |
| C49 | partial | Ngai Takakto2 | 193,700 | 96,850 | 1619097 | 6135520 |
| C50 | AUT.017559.02.01 | IJ & BM Broadhurst | 105,000 | 105,000 | 1619399 | 6134994 |
| C51 | AUT.016914.02.01 | I M Fulton-2 | 60,000 | 40,000 | 1619585 | 6134880 |
| C52 | AUT.029171.01.01 | J P Broadhurst | 24,000 | 24,000 | 1619442 | 6134796 |
| C53 | APP.038380.01.01 | Holloway* | 14,900 | 14,900 | 1619702 | 6134754 |
| C54 | AUT.029109.01.01 | I M Fulton-1 | 60,000 | 20,000 | 1619452 | 6134520 |
| C55 | APP.038328.01.01 | KB&SD Shine* | 39,200 | 39,200 | 1619411 | 6134224 |
| C56 | APP.038454.01.01 | Elbury Holdings-King* | 113,700 | 113,700 | 1619904 | 6133984 |
| C57 | AUT.027391.01.01 | Stanisich1 | 180,000 | 120,000 | 1618046 | 6133608 |
| C58 | APP.027391.01.02 | Stanisich-proposed* | 64,070 | 64,070 | 1617846 | 6133480 |
| C59 | APP.038420.01.01 | Matijevich2* | 193,700 | 96,850 | 1618003 | 6133379 |
| C60 | partial | Matijevich1 | 193,700 | 96,850 | 1617905 | 6132480 |
| C61 | APP.038650.01.01 | Hewitt* | 39,200 | 39,200 | 1617436 | 6132318 |
| C62 | AUT.038339.01.01 | Broadhurst | 50,000 | 50,000 | 1618994 | 6131326 |
| C63 | AUT.020533.02.01 | Luca Vista | 24,200 | 24,200 | 1619057 | 6130879 |
| C64 | AUT.038402.01.01 | Bell | 35,000 | 35,000 | 1619211 | 6130581 |
| C65 | AUT.036868.01.01 | Stanisich2 | 180,000 | 60,000 | 1618376 | 6129421 |
| C66 | AUT.003580.01.03 | Rangaunu | 35,000 | 35,000 | 1618726 | 6129089 |
| C67 | AUT.017045.01.02 | VALIC3 | 558,000 | 186,000 | 1616982 | 6128849 |
| C68 | AUT.004564.01.04 | Far North Farms Ltd | 80,000 | 80,000 | 1618816 | 6128564 |
| C69 | AUT.017045.01.02 | VALIC2 | 558,000 | 186,000 | 1616610 | 6128425 |
| C70 | AUT.003968.01.03 | DG&HA Inglis | 25,000 | 25,000 | 1618916 | 6128385 |
| C71 | AUT.017045.01.02 | VALIC1 | 558,000 | 186,000 | 1617061 | 6128196 |
| C72 | AUT.014520.02.01 | Millpara | 183,920 | 91,960 | 1617699 | 6128150 |

| Figure reference | IRISID (where available) | Bore Owners | Groundwater Take-Consented Total ($m^3$/yr) | Groundwater Take per Bore ($m^3$/yr) | X coordinate | Y coordinate |
|---|---|---|---|---|---|---|
| C73 | AUT.014520.01.02 | Millpara | 183,920 | 91,960 | 1617696 | 6127997 |
| C74 | AUT.002459.01.03 | Avocado Investments Ltd | 18,600 | 18,600 | 1617322 | 6126681 |
| C75 | AUT.008589.01.02 | RA&LS Huddart | 11,040 | 11,040 | 1617926 | 6126666 |
| C76 | AUT.003788.01.03 | Javo | 18,600 | 18,600 | 1617131 | 6126650 |
| C77 | AUT.004350.01.03 | Hayward | 24,000 | 24,000 | 1618191 | 6126546 |
| C78 | AUT.008177.01.02 | JB & GM Clark | 24,000 | 24,000 | 1618190 | 6126545 |
| C79 | AUT.003798.01.04 | NG Rouse | 16,500 | 16,500 | 1617423 | 6126357 |
| C80 | AUT.028476.01.01 | J Jones | 60,000 | 60,000 | 1618328 | 6125903 |
| C81 | AUT.004571.01.03 | DC&MA Olsen | 45,000 | 45,000 | 1619564 | 6125618 |
| P20 | APP.040130.01.01 | Tuscany | 36,000 | 36,000 | 1614331 | 6138447 |
| P21 | APP.040386.01.01 | Robert Campbell | 360,000 | 360,000 | 1615815 | 6135787 |
| P22 | APP.039841.01.02 | Yelavich | 52,000 | 52,000 | 1616834 | 6134008 |
| P23 | APP.040363.01.01 | Wataview | 33,750 | 33,750 | 1619441 | 6131282 |
| P24 | APP.040361.01.01 | Tiri | 581,250 | 290,625 | 1618056 | 6130290 |
| P25 | APP.040361.01.01 | Tiri | 581,250 | 290,625 | 1618856 | 6130196 |
| P26 | APP.040362.01.01 | Valic | 173,700 | 173,700 | 1617589 | 6129130 |

Table C3. Consented and proposed groundwater users in Northern portion of the model corresponding to Figure 9C

| Figure reference | IRISID (where available) | Bore Owners | Groundwater Take-Consented Total ($m^3$/yr) | Groundwater Take per Bore ($m^3$/yr) | X coordinate | Y coordinate |
|---|---|---|---|---|---|---|
| C82 | | Te Urungi O Ngati Kuri LTD | 18,250 | 18,250 | 1623319 | 6122860 |
| C83 | | Far North Holiday Park-Non irrigation | 10,920 | 10,920 | 1615677 | 6122797 |
| C84 | | J A Trussler | 148,800 | 148,800 | 1618833 | 6122488 |
| C85 | | FNDC: GW take for Kaitaia | 1,460,000 | 1,460,000 | 1618250 | 6121600 |
| C86 | | Sweetwater Farms_PB16 | 1,210,242 | 110,022 | 1616968 | 6121153 |
| C87 | | Sweetwater Farms_PB3 | 1,210,242 | 110,022 | 1616579 | 6120782 |
| C88 | | Sweetwater Farms_PB1 | 1,210,242 | 110,022 | 1617060 | 6120384 |
| C89 | | Landcorp Farming Limited | 200,000 | 200,000 | 1619617 | 6120296 |
| C90 | | Sweetwater Farms_PB2 | 1,106,760 | 598,000 | 1617891 | 6119767 |
| C91 | | Sweetwater Farms_PB7 | 1,210,242 | 110,022 | 1618481 | 6119718 |
| C92 | | KJ & FG King : GW for Awanui Straight-1 | 278,262 | 92,754 | 1622335 | 6119515 |
| C93 | | KJ & FG King : GW for Awanui Straight-3 | 278,262 | 92,754 | 1622365 | 6119515 |
| C94 | | Sweetwater Farms_PB5 | 1,210,242 | 110,022 | 1617613 | 6119386 |
| C95 | | Sweetwater Farms_PB10 | 1,210,242 | 110,022 | 1619652 | 6119162 |
| C96 | | Sweetwater Farms_PB4 | 1,210,242 | 110,022 | 1616934 | 6119154 |
| C97 | | KJ & FG King : GW for Awanui Straight-2 | 278,262 | 92,754 | 1622954 | 6119131 |
| C98 | | Sweetwater Farms_PB6 | 1,106,760 | 508,760 | 1617450 | 6119000 |
| C99 | | Sweetwater Farms_PB9 | 1,210,242 | 110,022 | 1618334 | 6118808 |
| C100 | | Sweetwater Farms_PB13 | 1,210,242 | 110,022 | 1618755 | 6118360 |
| C101 | | Sweetwater Farms_PB11 | 1,210,242 | 110,022 | 1617376 | 6118236 |
| C102 | | Sweetwater Farms_PB14 | 1,210,242 | 110,022 | 1617307 | 6117876 |
| C103 | | RF & MH Barber-Tudorwood Orchard | 23,760 | 23,760 | 1623509 | 6117021 |
| P27 | | Sweetwater-5 | 1,080,000 | 180,000 | 1617267 | 6121591 |
| P28 | APP.040364.01.01 | Elbury Holdings | 200,000 | 100,000 | 1618634 | 6121359 |
| P29 | APP.040364.01.02 | Elbury Holdings | 200,000 | 100,000 | 1618542 | 6121003 |
| P30 | | Sweetwater-4 | 1,080,000 | 180,000 | 1616465 | 6120787 |
| P31 | | Sweetwater-3 | 385,000 | 385,000 | 1617109 | 6120717 |
| P32 | | Sweetwater-6 | 1,080,000 | 180,000 | 1616868 | 6120002 |
| P33 | | Sweetwater-2 | 436,000 | 436,000 | 1617846 | 6119771 |
| P34 | | Sweetwater-1 | 632,000 | 632,000 | 1617473 | 6119002 |
| P35 | | Sweetwater-7 | 1,080,000 | 180,000 | 1617043 | 6118433 |
| P36 | | Sweetwater-9 | 1,080,000 | 180,000 | 1617279 | 6117495 |
| P37 | | Sweetwater-8 | 1,080,000 | 180,000 | 1616978 | 6116808 |

| Figure reference | IRISID (where available) | Bore Owners | Groundwater Take- Consented Total ($m^3$/yr) | Groundwater Take per Bore ($m^3$/yr) | X coordinate | Y coordinate |
|---|---|---|---|---|---|---|
| P38 | | Sweetwater-10 | 210,000 | 105,000 | 1617702 | 6114717 |
| P39 | | Sweetwater-11 | 210,000 | 105,000 | 1617254 | 6113920 |
| P40 | | Sweetwater-12 | 350,000 | 116,667 | 1616055 | 6112008 |
| P41 | | Sweetwater-13 | 350,000 | 116,667 | 1616563 | 6111903 |
| P42 | | Sweetwater-14 | 350,000 | 116,667 | 1616889 | 6111890 |

# Appendix D. Irrigation Scheduling and Actual Irrigation Use

## D.1 Development of an irrigation scheduling dataset

The irrigation module of Soil Moisture Water Balance Model was utilised to optimise irrigation applications for avocado orchards in the area and to provide input into the transient irrigation scenario for groundwater modelling purposes. The parameters and associated values used in the model are shown in **Table C1**.

Table C1. Summary of parameters used in the irrigation model

| Parameter | Description | Values | Basis of Values |
|---|---|---|---|
| Maximum Soil Moisture Content (ST) | The capacity of water in mm in the soil at field capacity. | 178.5 | Estimated from potential rooting depth (PRD) and macroporosity (n). ST = PRD x n/100.<br>1190 mm x 15%= 178.5 mm |
| Plant Available Water (PAW) | The amount of water physically accessible by the plants in the root zone in mm. | 125 | Table 22 of Crop Evapotranspiration - Guidelines for Computing Crop Water Requirements from the Food and Agricultural Organisation of the United Nations (FAO)[1] states that 70% of Total Available Soil Water (interpreted as equivalent to ST in the SMWBM) can be depleted before the point where avocado trees suffer stress. Therefore,<br>PAW = 0.7 x ST |
| Allowable Deficit (AD) | Soil moisture level where irrigation ceases. | 90% of PAW | The avocado is very flood-sensitive with even short periods of waterlogging resulting in reduced shoot growth, altered mineral uptake and root death. To avoid flooding and surface runoff, soil moisture levels during irrigation should not exceed 90% of field capacity. |
| Minimum/ Critical Deficit (CD) | Percentage of PAW at which further drying of soil would start to have an impact on plant growth rates, and hence CD represents the soil moisture level at which irrigation commences. | 40% of PAW | The rule of thumb for critical deficit is 50% of PAW. However, a grower aiming to maximise crop yield may want a small critical deficit of only 20% (80% PAW)[2]. A balance is also required between a small critical deficit (high soil moisture levels) and water wastage, which results under high moisture conditions when rainfall occurs during summer. Through trial and error, we have used CD values of 40% PAW. |
| Peak Application Depth | Maximum daily irrigation depth applied to soil (mm/day). | 4.0 mm | Selected through optimisation target of minimisation in losses, while maintaining moisture levels at or above the CD. Note. This is the amount of irrigation water reaching the soil surface, which is less that the amount applied by the irrigator *per se*. due to application inefficiencies (losses). |
| Application Duration | Duration in hours over which the peak application depth is applied | 2 hours | Data estimated |
| Rain Threshold | Daily rainfall total in mm when a farmer would choose not to irrigate. | 10 mm | Judgement |
| Season | Irrigation season start and finish | October – April | General irrigation season length. |

The historical rainfall record from 01/01/1960 to 31/07/2018 was used in the model. The simulated soil moisture content with/without irrigation are shown in **Figure C1**.

1 http://www.fao.org/docrep/x0490e/x0490e0e.htm
2 Anon. Scheduling overview. NZ Avocado Industry 11 Mar 2010. (accessed 16 Jul 2015) <http://www.hortinfo.co.nz/factsheets/fs110-68.asp>.

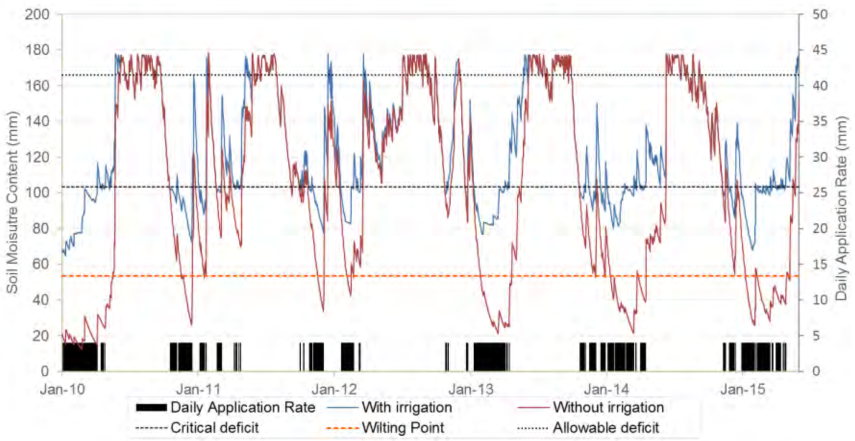


Figure C1. Irrigation simulation output for time period 2010-2015

The daily peak application rate was optimised through a set of simulations, aiming to minimize the water losses through surface runoff and percolation to groundwater system, while maintaining a soil moisture content that is above the plant critical deficit.

The simulations indicate an optimized peak application rate of 4 mm/day. The relationship between annual irrigation amount and peak application rate is shown in **Figure C2**.

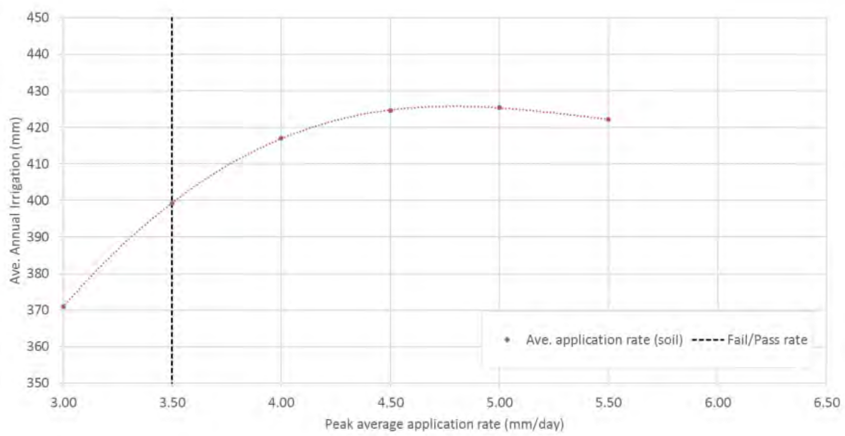


Figure C2. Assessment of peak application rate that is water conservative for sandy soils.

The irrigation demand was simulated for the period of 01/01/1960 to 31/07/2018 and a summary graph showing the number of days irrigation was required per season is shown in **Figure C3**.

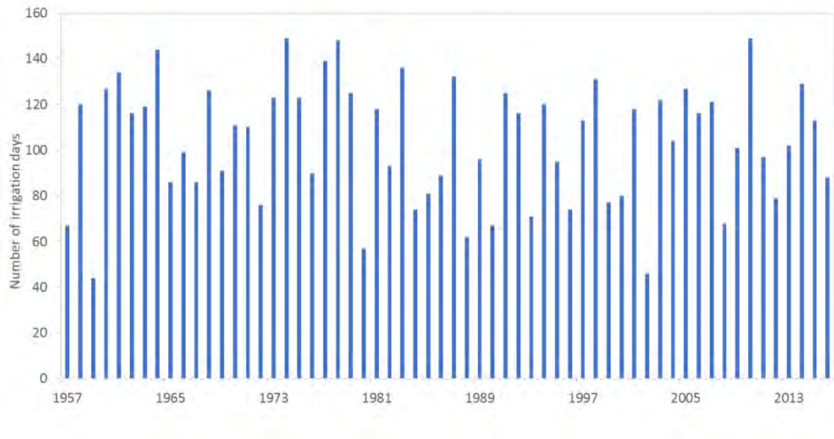


Figure C3. Simulated number of irrigation days per season.

The statistical distribution of monthly irrigation application totals, with 10% additional water added to account for irrigation inefficiency, is shown in **Figure C4**.

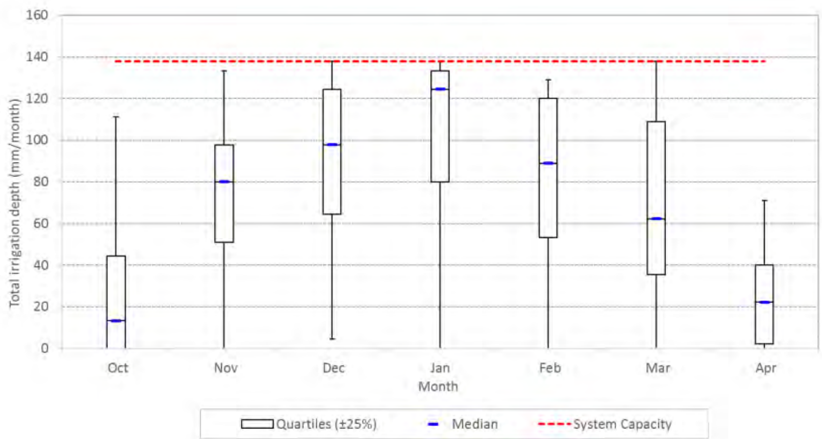


Figure C4. Seasonal irrigation demand for sandy soil.

The annual irrigation demand volume and commensurate number of days of irrigation was calculated and it was found that the 90%ile of simulated annual demand is equivalent to approximately 150 days pumping at the peak rate. This closely aligns with the annual volumes specified in consents granted.

## D.2 Development of an irrigation actual use dataset

The simulated irrigation demand time series was applied to one of the currently consented groundwater bores with a peak allocation rate of 720 $m^3$/day owned by Ivan Stanisich (NRC consent No. CON20102739101). The total amount of demand simulated during the irrigation period was calculated and compared with available historical use records, as shown in **Figure C5**.

The simulated demand varies with climate conditions from a minimum of 44 days irrigation to a maximum of 149 days irrigation during the irrigation season. For the years where records were available for comparison, measured demand is approximately 30% of simulated demand. There are a number of minor reasons for this including human operational decision and actual rainfall not being totally consistent with site rainfall, but the primarily reason is that the orchard is not fully developed.

Considering the scope and purpose of this modelling, this irrigation demand time series is a conservative estimate and therefore appropriate to use in effects assessment from the abstraction of groundwater.

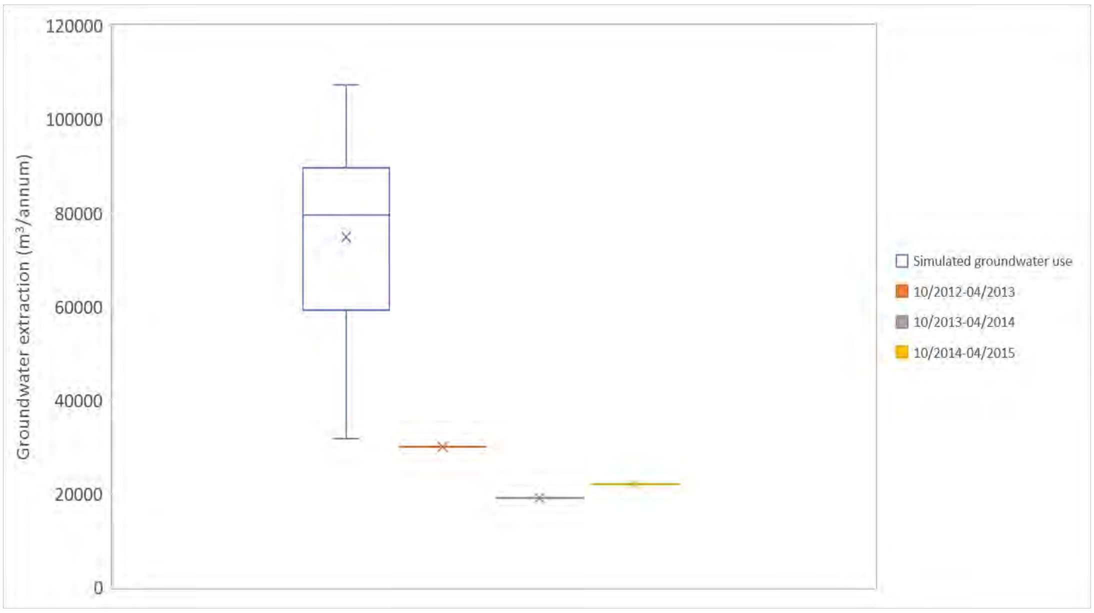


Figure C5. Comparison between the simulated groundwater demand and the historical records.

The irrigation demand pattern from **Section C.1** was applied to all the groundwater irrigation bores in the model area to construct transient pumping time series input for the model.

# Appendix E. Calibrated Model Hydrographs

Waterfront (19 m)

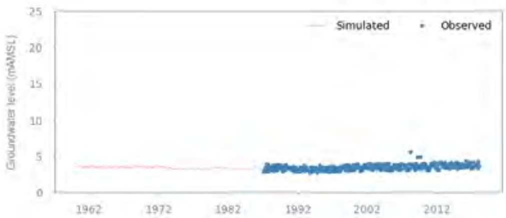


Waterfront (37 m)

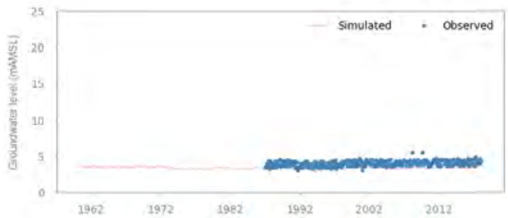


Waterfront (57 m)

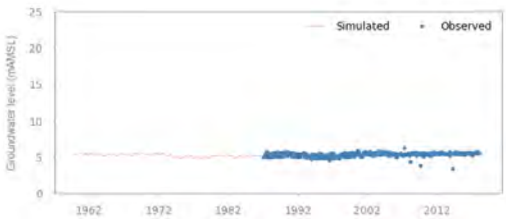


Waterfront (74 m)

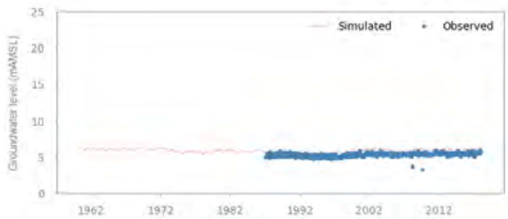


Fishing Club (78 m)

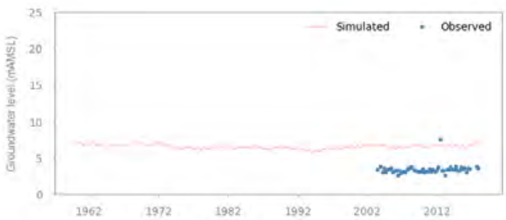


Wagener (69 m)


Browne (16 m)

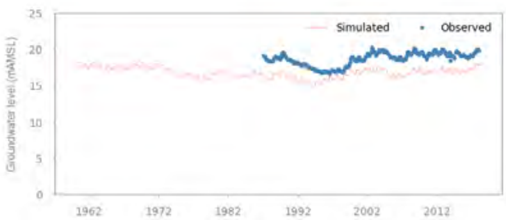


Browne (29 m)

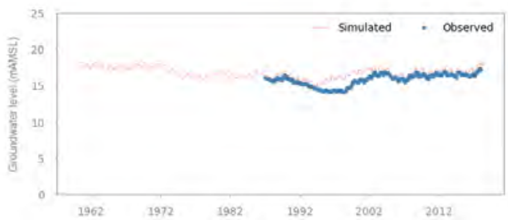


Browne (59 m)

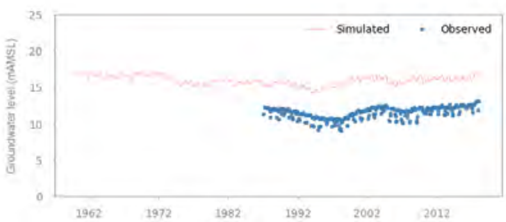


Forest (16 m)

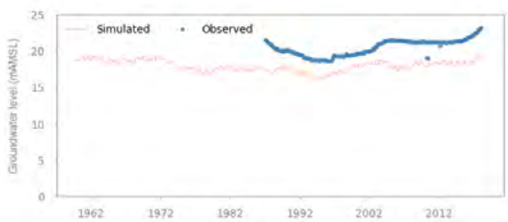

Forest (36 m)

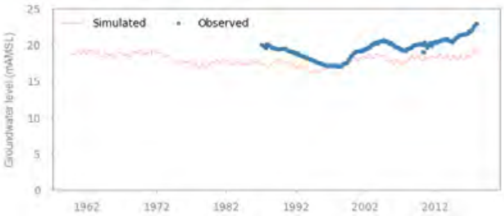


Forest (64 m)

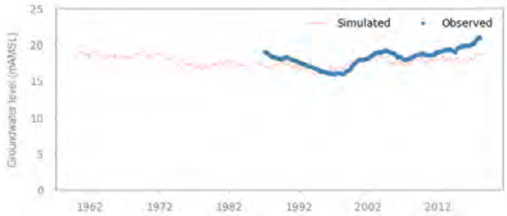


Forest (79 m)

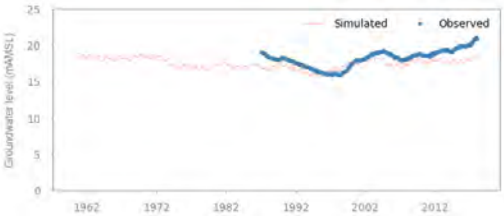


Hukatere (19 m)

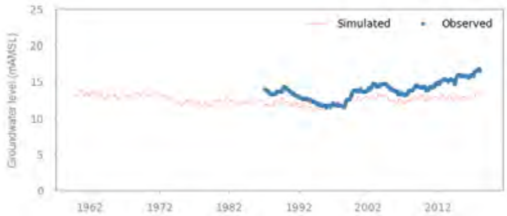


Hukatere (36 m)


Hukatere (58 m)


Kaimaumau Deep (72 m)

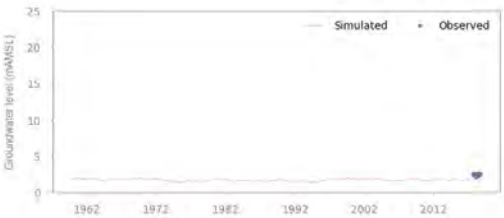


Paparore (18 m)

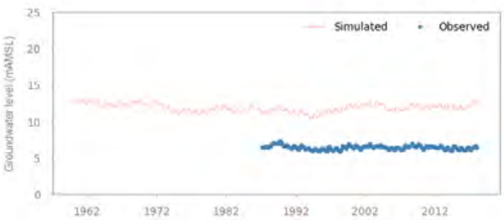


Paparore (35 m)

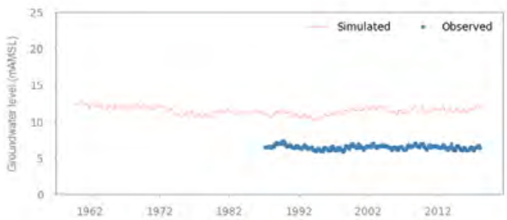

Paparore (65 m)

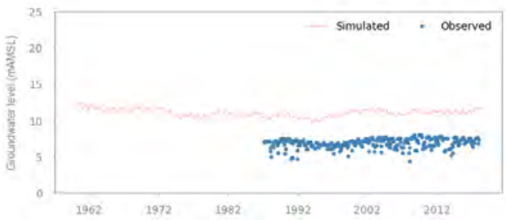


Paparore (75 m)

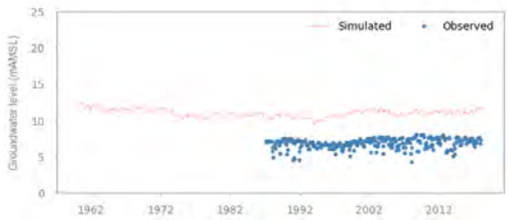


Ogle Drive (68 m)


Valic-1 (Shallow Monitoring-17 m)

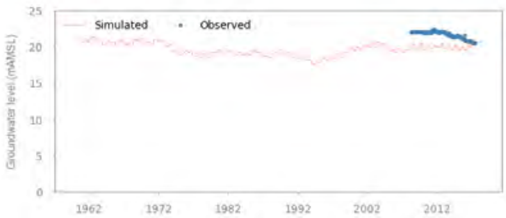


Valic-1 (Deep Monitoring-103 m)


Valic-1 (Production Bore-103 m)

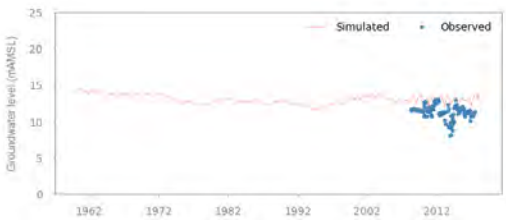

Valic-2 (Shallow Monitoring-55 m)


Valic-2 (Deep Monitoring-121 m)

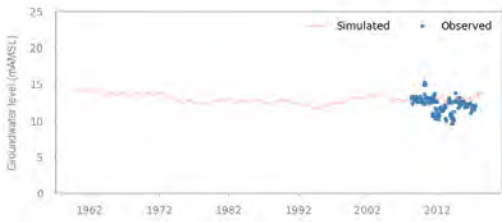


Valic-2 (Deep Production-121 m)


Valic-3 (Shallow Monitoring-45 m)


Valic-3 (Deep Monitoring-124 m)


Valic-3 (Deep Production-124 m)

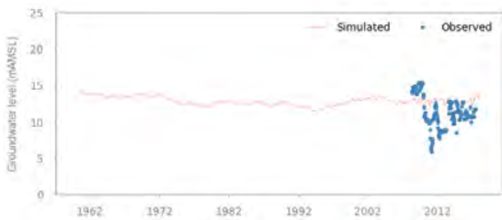

Valic-4 (Shallow Monitoring-13 m)

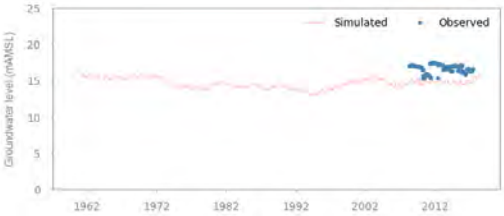


Valic-4 (Deep Monitoring-93 m)


Valic-4 (Deep Production-93 m)


Sweetwater MW1 (13 m)


Sweetwater MW1 (94 m)


Sweetwater MW2 (15 m)


Sweetwater MW2 (59 m)

Sweetwater MW3 (5 m)


Sweetwater MW3 (47 m)

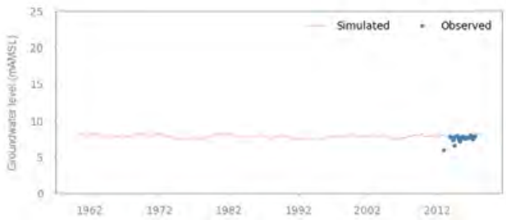


Sweetwater MW4 (25 m)

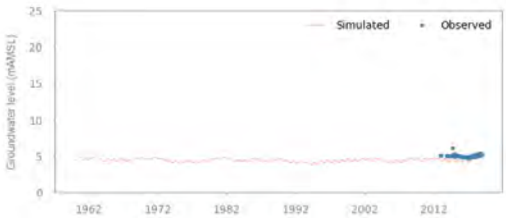


Sweetwater MW4 (92 m)


Sweetwater MW5 (6 m)

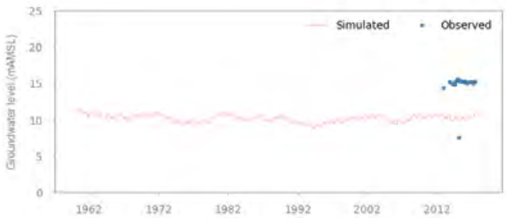


Sweetwater MW5 (61 m)

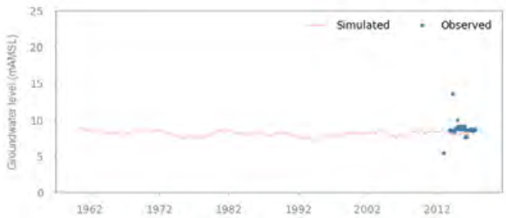


Sweetwater MW6 (15 m)

Sweetwater Nursery (34 m)

Waipapa (56 m)


Shanks (Unknown depth)

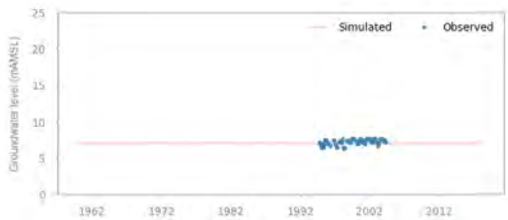


Vinac (33 m)

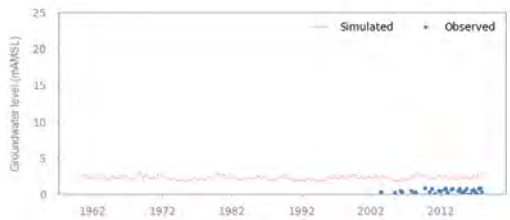


Matich (Unknown depth)

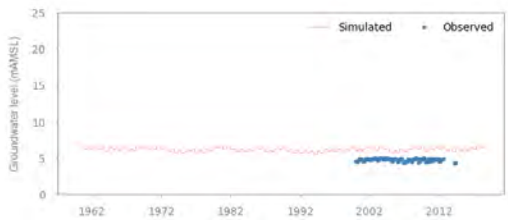


Welch (32 m)

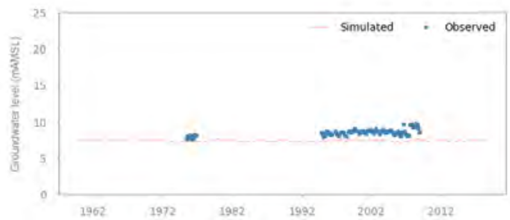


Lake Heather 1 (26 m)

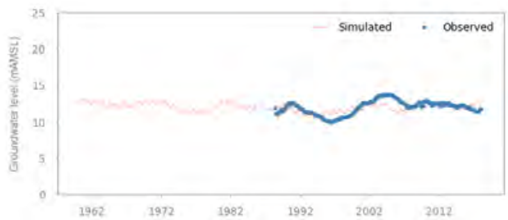


Lake Heather 1 (105 m)

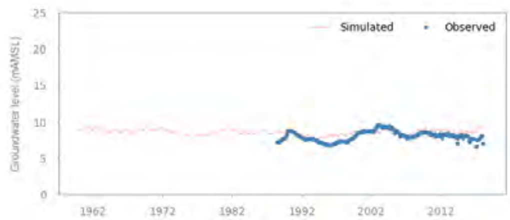

Lake Heather 2 (29 m)

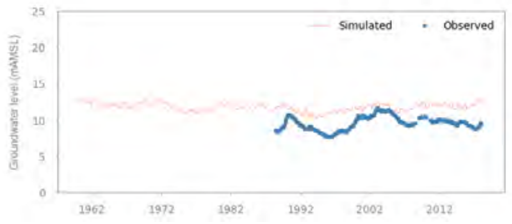


Lake Heather 3 (29 m)

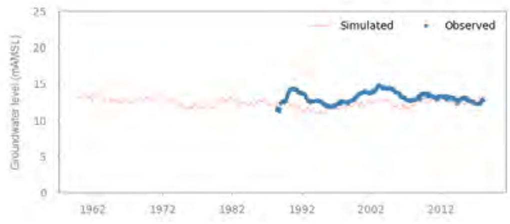


Figure E1. Hydrographs of simulated versus observed groundwater levels.